BMC Cancer

RESEARCH Open Access

Integrated bulk and single-cell profiling characterize sphingolipid metabolism in pancreatic cancer

Biao Zhang[1†], Bolin Zhang[2†], Tingxin Wang[1,3†], Bingqian Huang[1,3], Lijun Cen[4,5*] and Zhizhou Wang[1*]

Abstract

Background Abnormal sphingolipid metabolism (SM) is closely linked to the incidence of cancers. However, the role of SM in pancreatic cancer (PC) remains unclear. This study aims to explore the significance of SM in the prognosis, immune microenvironment, and treatment of PC.

Methods Single-cell and bulk transcriptome data of PC were acquired via TCGA and GEO databases. SM-related genes (SMRGs) were obtained via MSigDB database. Consensus clustering was utilized to construct SM-related molecular subtypes. LASSO and Cox regression were utilized to build SM-related prognostic signature. ESTIMATE and CIBERSORT algorithms were employed to assess the tumour immune microenvironment. OncoPredict package was used to predict drug sensitivity. CCK-8, scratch, and transwell experiments were performed to analyze the function of ANKRD22 in PC cell line PANC-1 and BxPC-3.

Results A total of 153 SMRGs were acquired, of which 48 were linked to PC patients' prognosis. Two SM-related subtypes (SMRGcluster A and B) were identified in PC. SMRGcluster A had a poorer outcome and more active SM process compared to SMRGcluster B. Immune analysis revealed that SMRGcluster B had higher immune and stromal scores and CD8 + T cell abundance, while SMRGcluster A had a higher tumour purity score and M0 macrophages and activated dendritic cell abundance. PC with SMRGcluster B was more susceptible to gemcitabine, paclitaxel, and oxaliplatin. Then SM-related prognostic model (including ANLN, ANKRD22, and DKK1) was built, which had a very good predictive performance. Single-cell analysis revealed that in PC microenvironment, macrophages, epithelial cells, and endothelial cells had relatively higher SM activity. ANKRD22, DKK1, and ANLN have relatively higher expression levels in epithelial cells. Cell subpopulations with high expression of ANKRD22, DKK1, and ANLN had more active SM activity. In vitro experiments showed that ANKRD22 knockdown can inhibit the proliferation, migration, and invasion of PC cells.

†Biao Zhang, Bolin Zhang and Tingxin Wang contributed this research equally.

*Correspondence:
Lijun Cen
810509659@qq.com
Zhizhou Wang
wangzhizhou@dmu.edu.cn

Full list of author information is available at the end of the article

Conclusion This study revealed the important significance of SM in PC and identified SM-associated molecular subtypes and prognostic model, which provided novel perspectives on the stratification, prognostic prediction, and precision treatment of PC patients.

Keywords Sphingolipid metabolism, Pancreatic cancer, Prognosis, Tumour microenvironment, Therapy, Single-cell analysis

Introduction

Pancreatic cancer (PC) is an increasingly prevalent tumour in the United States, ranking as the fourth-highest contributor to cancer-related mortality. The incidence of this disease is progressively on the rise among both male and female populations [1]. A crucial problem in treating PC is the difficulty of diagnosis at early stages (i.e., T1 and T2 tumours), which typically exhibit no symptoms. The majority of PC (80%) are detected in the advanced stage (i.e., T3 and T4 tumours with lymph nodes and distant metastases), resulting in lost opportunities for curative surgery [2–4]. Furthermore, the treatment of PC faces a critical problem of high resistance and poor response to anticancer drugs and radiotherapy [5]. The combination of limited treatment options and late detection contributes to PC being one of the deadliest cancers. Despite more advanced surgery and more potent anticancer drugs that have been developed recently, these developments in therapy have not resulted in appreciably higher overall survival rates [6–8]. Only 11% of PCs survive for five years, the lowest among all cancers [1]. Therefore, investigating novel diagnostic and prognostic biomarkers that can facilitate early detection and treatment strategies for this disease is imperative.

In recent years, extensive research has been conducted on bioactive lipids, particularly sphingolipids, revealing a strong association between lipidome and human diseases [9–11]. Sphingolipids serve as structural and functional components of the cell membrane, including sphingosine-1-phosphate (S1P), ceramide, sphingosine, and sphingomyelin. And enzymes involved in sphingolipid metabolism (SM) include sphingosine kinase (SPHK), sphingomyelinase, and ceramidase [12]. Research indicated that aberrant SM might play a critical role in the incidence of various malignant tumours [13]. Sphingolipid production and degradation frequently exhibit abnormalities in cancer cells, leading to modifications in the composition as well as properties of cellular membranes. These changes can influence critical biological processes like cell signaling, cell adhesion, and apoptosis, ultimately facilitating the progression of cancers. By regulating cancer cell signal transduction networks, sphingolipids control a range of complex biological processes [14, 15]. For example, ceramide and S1P, two bioactive lipids, have opposing roles as tumour suppressors and tumour promoters, respectively [16]. Understanding sphingolipid metabolism is crucial in deciphering the mechanisms underlying cancer cell death and survival, particularly in response to anticancer treatments [17]. Some breakthroughs have been made in the field of digestive tract tumours and even PC by targeting downstream components of SM and related signal transduction [18, 19]. For instance, Zhang et al. discovered that ceramide-1-phosphate transfer protein could stimulate the metastasis of PC cells through the regulation of ceramide and PI4KA/AKT signaling pathway [19]. Furthermore, the key enzymes and intermediates of SM have emerged as crucial regulators of tumour cells, influencing clinical prognosis. Consequently, they are increasingly recognized as promising themes in the development of novel anticancer therapies.

This study explored the role of SM-related genes (SMRGs) in PC prognosis and built SM-associated molecular subtype, which is linked to the clinical pathological features, prognosis, immune microenvironment, and treatment response. Furthermore, a prognostic risk prediction model related to SM was built, which had good prediction performance. Single-cell analysis revealed the cell subsets in PC microenvironment and the activity of SM in each cell subset. These results presented new targets and tactics for PC patients' stratification and precision treatment.

Materials and methods

Data gathering

The transcript and clinical data (including a total of 185 PCs) were collected in The Cancer Genome Atlas (TCGA, https://portal.gdc.cancer.gov/). GSE62452 (co ntaining 69 cases of pancreatic tumour and 61 cases of adjacent tissues), GSE28735 (containing 45 cases of pancreatic tumour and adjacent tissues), GSE85916 (containing 80 cases of pancreatic tumour tissues), and GSE57495 (containing 63 cases of pancreatic tumour tissues) datasets were collected in Gene Expression Omnibus (GEO, https://www.ncbi.nlm.nih.gov/geo/). Employing the "sva" package to process transcript data across entirely distinct datasets to make them balanced and consistent [20, 21]. The SM-related gene sets were collected in The Molecular Signatures Database (MSigDB, http://www.gsea-msigdb.org/) [22]. The univariable Cox regression with a p-value less than 0.05 was utilized to screen SMRGs associated with PC prognosis. Copy number variation (CNV), single nucleotide variation (SNV), as well as methylation information of various cancers in TCGA platform, were

obtained for investigating the genetic changes of the prognostic SMRGs in pan-cancer.

Consensus clustering

The transcriptome data of PCs derived from different datasets was merged. Then, consensus clustering was implemented utilizing "ConsensusClusterPlus" package [23]. The ideal clustering results were identified from the cumulative distribution function (CDF) curve. To further illustrate the reliability of clustering results, principal component analysis (PCA) and t-distributed stochastic neighbour embedding (t-SNE) were carried out [24]. Single-sample gene set enrichment analysis (ssGSEA) was implemented to evaluate the changes in SM-associated signaling pathways between different molecular subtypes. In addition, gene set variation analysis (GSVA) and GSEA were implemented to investigate the underlying mechanisms of variations between the various molecular subtypes [25].

Immunoassay and drug sensitivity

The ESTIMATE algorithm was employed for calculating stromal, immune, and tumour purity scores between different subtypes [26]. For further comparing the infiltrated level of immune cell subpopulation in tumour microenvironment between various subtypes, the CIBERSORT algorithm was employed for assessing the infiltrated proportion of 22 immune cell subpopulations [27]. The p-value < 0.05 indicated that the infiltrated proportion generated by CIBERSORT was accurate, which was utilized in subsequent analysis. OncoPredict package can predict the half maximal inhibitory concentration (IC50) value of the drug utilizing the sample's gene expression data, which was used in this study to compare drug sensitivity between various subgroups [28].

Enrichment analysis

The "limma" package was employed for identifying the differentially expressed genes (DEGs) among various subtypes, with a selection criterion of |log2 fold change (FC)| > 1 and an adjusted p-value < 0.05. These DEGs were identified as SM-associated DEGs. Gene Ontology (GO) and Kyoto Encyclopedia of Genes and Genomes (KEGG) enrichment analyses were implemented to explore the biological behaviours that SM-associated DEGs participated in [29, 30].

Building of SM-related prognostic model

In this study, LASSO and Cox regression analyses were implemented to develop a prognostic model for PC utilizing SM-related DEGs [31–33]. The "caret" function was utilized to split PCs from TCGA into training as well as internal validation sets at a 5:5 ratio. The external validation was completed utilizing PCs from the GEO database. Each sample could be classified into a high- or low-risk population via comparison with the median value of risk score in the training set. Kaplan-Meier (KM) approach was employed for comparing the prognosis in various risk groups [34]. The time-dependent receiver operating characteristic (ROC) curve and area under the curve (AUC) were employed to assess the model's prediction efficiency [35].

Model gene expression analysis

GSE62452 and GSE28735 datasets were utilized to investigate the RNA expression levels of ANLN, ANKRD22, and DKK1 in PC. UALCAN platform (https://ualcan.path.uab.edu) can perform differential expression analysis based on tumour proteome data from the CPTAC database [36]. It was employed for investigating the protein expression levels of ANLN, ANKRD22, and DKK1 in PC. Human Protein Atlas (HPA) is a public website (https://www.proteinatlas.org) that provides immunohi stochemical results of tumour patients [37]. It was used to download immunohistochemistry pictures of ANLN, ANKRD22, and DKK1 in PC.

Construction of protein-protein interaction (PPI) and competitive endogenous RNA (ceRNA) networks

STRING platform (https://cn.string-db.org/) was utilize d to explore molecular proteins that interact with model genes, and the minimum interaction score was set to 0.4 [38]. The miRDB (https://mirdb.org/), TargetScan (https://www.targetscan.org/vert_80/), miRanda (https://mirdb.org/), miRWalk (http://mirwalk.umm.uni-heidelberg.de/)were utilized to search for miRNAs that regulate model genes, then the miRNAs obtained from the four platforms were intersected [39]. The spongeScan (http://spongescan.rc.ufl.edu) platform was used to find lncRNAs that have a regulatory relationship with miRNAs [40, 41]. PPI and ceRNA networks were visualized using Cytoscape software (version 3.9.1).

Single-cell analysis

Single-cell RNA sequencing (scRNA) data was collected from GSE214295 dataset (containing three PC tissues) in GEO platform. Utilizing the "Seurat" package (version 4.3.0), scRNA data of PC samples were converted into Seurat object and then merged [42, 43]. Filter conditions were set as below: each gene was expressed in a minimum of three cells, each cell expressed more than 200 genes, and the proportion of mitochondrial genes was under 20%. The "NormalizeData" function was Employed to normalize scRNA data. After PCA utilizing the first 2000 hypervariable genes, "Harmony" function was employed to remove batch effects among various tissues and dimensionality reduction. "FindNeighbors" and "FindClusters" functions were employed to assess the

similarity between cells and cluster cell subpopulations. UMAP was utilized for visualization [44]. Then cells were annotated using "Human Primary Cell Atlas" [45]. Intercellular communication was analyzed via "CellChat" package (version 1.6.1). SM score was evaluated utilizing "UCell", "singscore", and "AddModuleScore" methods.

Real-time quantitative PCR

The total RNAs were isolated utilizing three cell lines (containing one type of pancreatic ductal epithelial cell: HPDE6-C7; two types of PC cells: BxPC3, PANC-1). Then, real-time quantitative PCR was implemented to detect the expressed levels of RNA, which were quantified using ΔΔCt technique. GAPDH served as an internal reference [46]. All the primer sequences for humans were acquired from GenePharma (Suzhou, China) and shown in Table S1.

Cell culture and siRNA transfection

PANC-1 and BxPC-3 cells were maintained in Dulbecco's Modified Eagle Medium (DMEM) and RPMI-1640 medium, respectively, both supplemented with 10% fetal bovine serum (FBS) (Gibco, USA). The cultures were incubated at 37 °C in an atmosphere of 5% CO2. siRNA designed to target ANKRD22 was transfected into the cells following the manufacturer's protocol (GenePharma, Suzhou, China).

CCK-8 experiment

PANC-1 and BxPC-3 were grown in 96-well plates. On hours 0, 24, 48, and 72, these cells were incubated with 100 μL of medium containing 10% CCK-8 reagent and incubated at 37 °C in the dark for 2 h. Subsequently, the OD values at 450 nm were measured to evaluate cell proliferation ability.

Scratch experiment

PANC-1 and BxPC-3 were seeded in 6-well plates and subjected to a scratch using a 200 μL pipette tip when they reached approximately 100% confluence. Photographs were captured on hours 0 and 24, and the scratched area was analyzed with ImageJ software. The healing rate of the scratch, reflecting cell migration ability, was calculated by taking the difference between the area on hour 0 and 24, divided by the area on hour 0.

Transwell invasion experiment

PANC-1 and BxPC-3 were cultured utilizing 100 μL of serum-free medium in a transwell chamber (Corning, NY, USA) pre-coated with Matrigel. In the lower chamber, 800 μL of medium supplemented with 10% FBS was added. After 24 h, the cells that migrated through the transwell chamber were counted to evaluate their invasion capability.

Data analysis

All data analysis was done utilizing GraphPad Prism 9 and R software (version 4.1.2). When measuring data had a normal distribution, the variation in the two groups was assessed utilizing a t-test. When measurement data didn't follow a normal distribution, the variation in the two groups was assessed utilizing the Wilcoxon test. The survival curve was drawn utilizing the KM approach. The p-value < 0.05 demonstrated statistical significance.

Results

Identification and analysis of SMRGs

The overall process of the study is displayed in Fig. 1. Based on MSigDB, 17 SM-related gene sets (containing 153 SMRGs) were obtained, of which 6 were derived from the GO database, 1 were derived from the KEGG pathway database, 2 were derived from the Reactome database, and 8 were derived from the WikiPathways database (Table S2). Univariable Cox regression analysis found that 48 SMRGs were linked to PC patients' prognosis, 19 SMRGs of which were linked to better prognosis (ST8SIA5, GPR6, B3GALT1, PLA2G6, SIRT3, GBA2, ABCA2, SMPD1, GLTPD2, ST6GALNAC6, SUMF2, SMPD2, SPHK2, ARSA, DEGS2, FUT1, B3GALT2, ABCB1, ST8SIA3), and 29 SMRGs were linked to poor prognosis (FUT3, FA2H, ALDH3B2, SGPP2, ARSI, SPHK1, UGCG, NAGA, ARSJ, STS, ESYT2, ESYT3, B4GALT1, SGMS2, ALDH3B1, PRKD3, PPP1CA, SPTLC2, ST3GAL1, SPTLC1, B3GNT5, PRKAA1, ABCC1, KDSR, CDK2, MTOR, SPTLC3, PITPNB, MAPK1) (Fig. 2A). Based on these prognostic SMRGs, PCA and t-SNE could clearly distinguish PC tissues from normal tissues in GSE28735 dataset (Fig. 2B and C) as well as GSE62452 dataset (Fig. 2D and E). Subsequently, we conducted further analysis of the expression differences of these prognostic SMRGs between PC and normal tissues. Most prognostic SMRGs exhibited significantly different expression levels, with SPTLC1, SGPP2, SGMS2, KDSR, PPP1CA, UGCG, SPHK1, SPTLC2, CDK2, B4GALT1, NAGA, B3GNT5, FUT3, ST3GAL1, STS, ALDH3B1, FA2H, ABCC1, PRKAA1, ARSJ, and ESYT2 being markedly upregulated in PC, while FUT1, B3GALT2, B3GALT1, ST8SIA5, ST6GALNAC6, ST8SIA3, GLTPD2, and PLA2G6 showed significantly reduced expression in PC tissues (Figure S1). These results suggest that SMRGs may be closely linked to PC occurrences and could be used as a potential diagnostic marker for PC.

Pan-cancer analysis

Abnormal SM is associated with tumorigenesis, so the genetic alteration of SMRGs in pan-cancer was explored in this study, including CNV, methylation, and SNV. Results found that CNV of SMRGs was a common

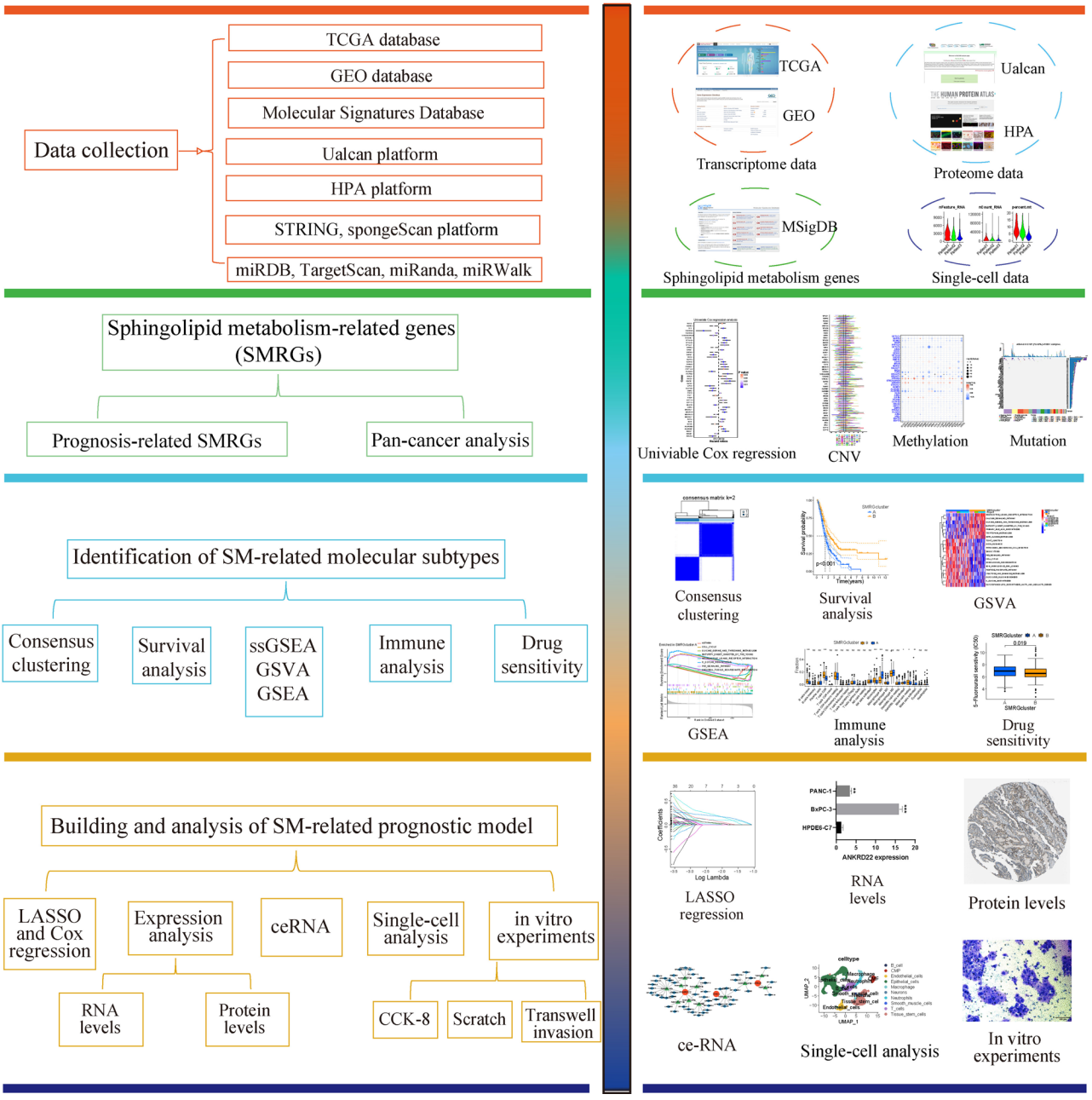

Fig. 1 The flow chart of this study

genetic change in 33 cancers, among which the CNV types of SPTLC3, SPHK1, B3GNT5, ST3GAL1, SUMF2, ABCB1, ESYT2, and ESYT3 were mainly manifested as gains, while the CNV types of SGMS2, SMPD1, and SIRT3 were mainly manifested as losses (Fig. 3A). Moreover, it was discovered that in most SMRGs, such as SPTLC1, KDSR, GBA2, PAPK1, SUMF2, PITPNB, and PIKAA1, there was a positive association between CNV and gene expression (Fig. 3B). Methylation is an epigenetic modification that can affect gene expression and the development of various cancers. This study indicated that the methylation level of ST8SIA5 and ST8SIA5 was higher within tumour tissues, while the methylation level of B3GALT1, FUT3, SPTLC3, and SGMS2 was higher within normal tissues (Fig. 3C). Correlation analysis revealed an intricate association of methylation and gene expression, with a positive correlation in B3GALT1, MTOR, CDK2, and SPTLC3 and a negative correlation in GLTPD2, FUT3, and KDSR (Fig. 3D). In addition, genetic mutations, such as TP53 and KRAS, have significant effects on gene expression and function and are directly associated with various cancers occurrence.

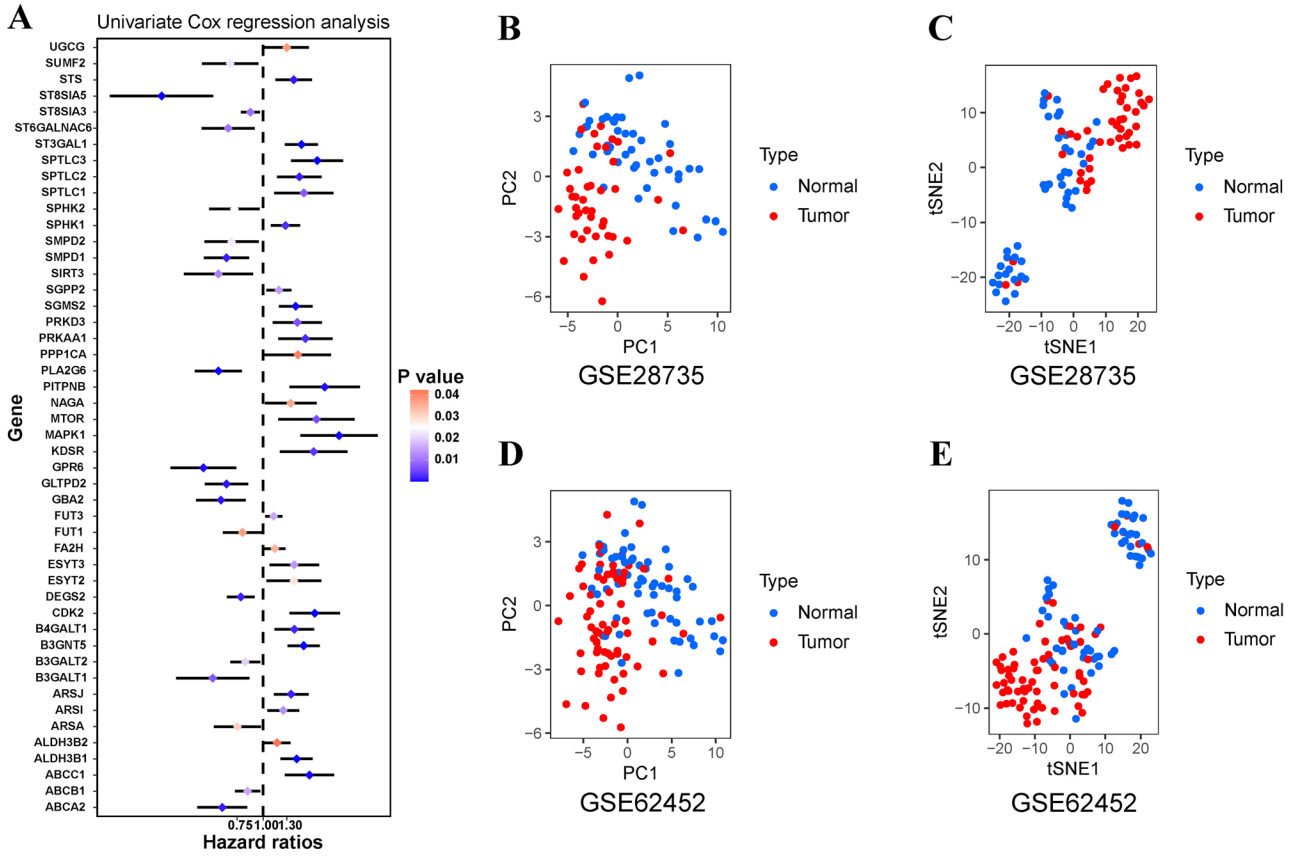

Fig. 2 Identification and analysis of prognostic-associated sphingolipid metabolism genes. **(A)** Forest map of prognostic-associated sphingolipid metabolism genes screened by univariable Cox regression. PCA **(B)** and t-SNE **(C)** could distinguish pancreatic tumour tissues from normal tissues in GSE28735 dataset. PCA **(D)** and t-SNE **(E)** could distinguish pancreatic tumour tissues from normal tissues in GSE62452 dataset

This study investigated SNV of SMRG in 33 kinds of cancers. MTOR, ABCB1, ABCA2, and ABCC1 were the top four genes in pan-cancer with the highest SNV frequency (Fig. 4A). Among the 33 cancers, skin cutaneous melanoma (SKCM) and uterine corpus endometrial carcinoma (UCEC) had a relatively higher overall mutation frequency of SMRGs (Fig. 4B).

Identification of SM-related molecular subtypes

To further explore the role of SM in PC, we identified the molecular subtypes related to SM in PC. Two SM-associated molecular subtypes (SMRGcluster A and SMRGcluster B) were identified for PC (Fig. 5A-C). PCA and t-SNE allowed for a clear distinction in various subtypes (Fig. 5D and E), which further demonstrated that clustering results were reliable. KM curves indicated a substantial variation between the two subtypes' prognoses, and SMRGcluster A patients' prognoses were noticeably worse than those of SMRGcluster B patients (Fig. 5F). In addition, the relationship between SM-related subtypes and pathological features of PC was analyzed in this study. The results showed that there was a higher proportion of the higher T, N, M, clinical stage, and pathological grade in SMRGcluster A patients compared with SMRGcluster B (Fig. 5G-K).

ssGSEA, GSVA, GSEA, and immunoassays

The ssGSEA was utilized to analyze the SM difference in various subtypes, result manifested that SMRGcluster A had a remarkably higher SM score (Fig. 6A). The underlying mechanisms of the differences in various subtypes were investigated utilizing GSVA and GSEA. We found that "p53 signaling pathway", "cell cycle", "homologous recombination", "glycolysis gluconeogenesis", and "O-glycan biosynthesis" were significantly enriched within SMRGcluster A. While "neuroactive ligand receptor interaction" and "calcium signaling pathway" were obviously enriched within SMRGcluster B (Fig. 6B and C).

Additionally, the difference in various PC patients is also closely related to tumour microenvironment heterogeneity. Based on "ESTIMATE" algorithm, it was found that SMRGcluster B had higher immune as well as stromal scores, while SMRGcluster A had a higher tumour purity score (Fig. 6D-F). CIBERSORT algorithm was further utilized to assess the infiltration abundance of 22 kinds of immune cell subpopulations in PC

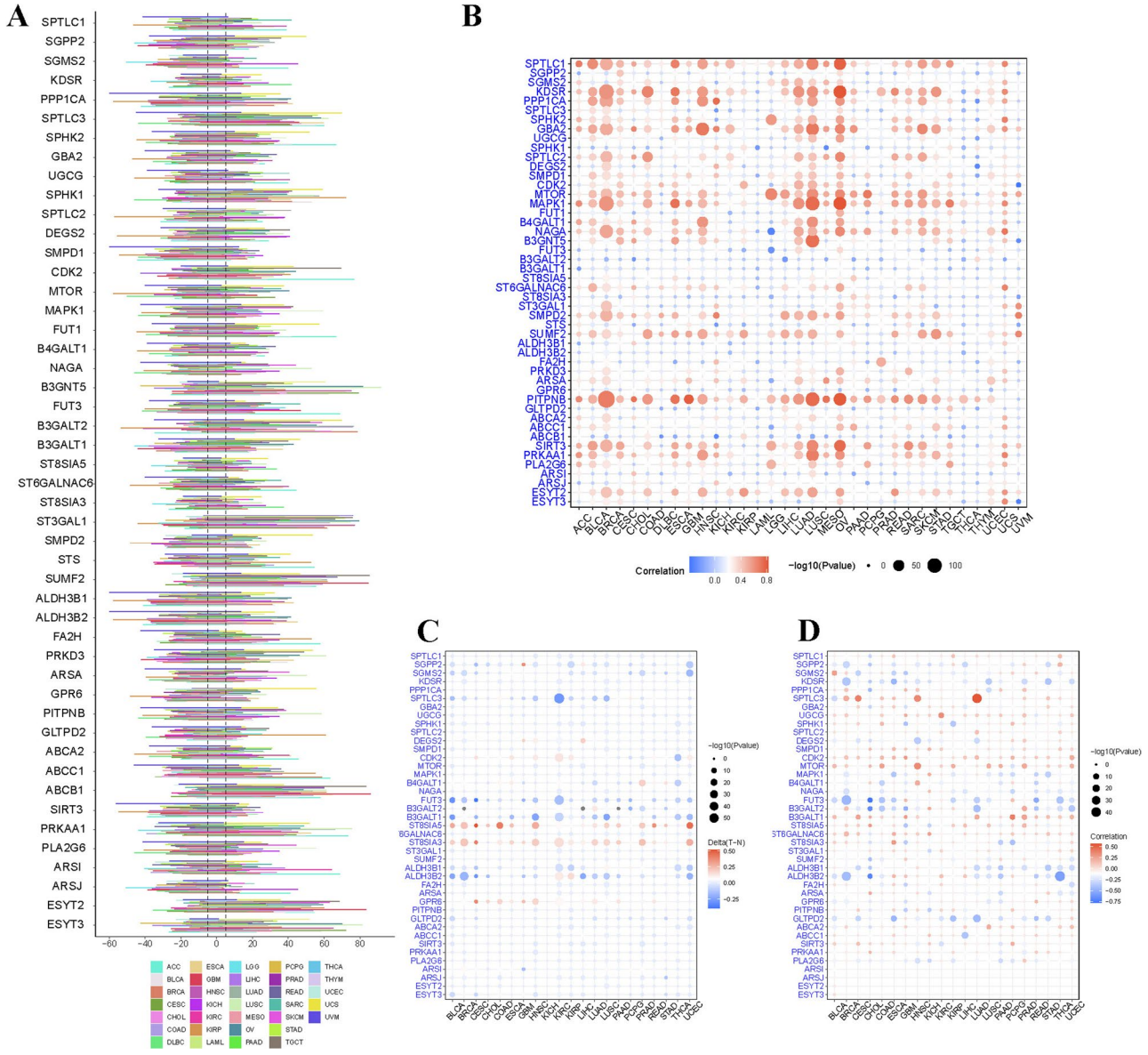

Fig. 3 Copy number variation (CNV) and methylation of sphingolipid metabolism-related genes (SMRGs) in pan-cancer. **(A)** CNV frequency of SMRGs in 33 kinds of cancers. **(B)** Correlation between CNV and expression of SMRGs in various cancers. **(C)** Differences in methylation levels of SMRGs between tumour and normal tissues. **(D)** Correlation between methylation and expression of SMRGs in various cancers

microenvironment. Results indicated that the infiltrated level of naïve B cells and CD8+T cells were higher in SMRGcluster B, while M0 macrophages and activated dendritic cells (DCs) had higher infiltration levels in SMRGcluster A (Fig. 6G).

Drug sensitivity between SM-related molecular subtypes

In addition to surgery, drug treatment is important for cancer patients and can improve their survival time. However, because different patients respond differently to drug treatment, the effectiveness of drug treatment is variable. To better assist the individualized treatment of PC patients, this study predicted the IC50 of anti-cancer drugs in various SM-associated subtypes. It was discovered that SMRGcluster A was more sensitive to sapitinib and selumetinib, and SMRGcluster B had a higher sensitivity to 5-fluorouracil, cisplatin, docetaxel, epirubicin, gemcitabine, irinotecan, oxaliplatin, paclitaxel, savolitinib, and sorafenib (Fig. 7A-L).

GO and KEGG enrichment analyses

To further seek the molecular targets related to the pathogenesis and prognosis of PC, 292 differentially expressed genes (DEGs) defined as SM-related DEGs were further identified between the various subtypes, of which 170 were highly expressed in SMRGcluster A

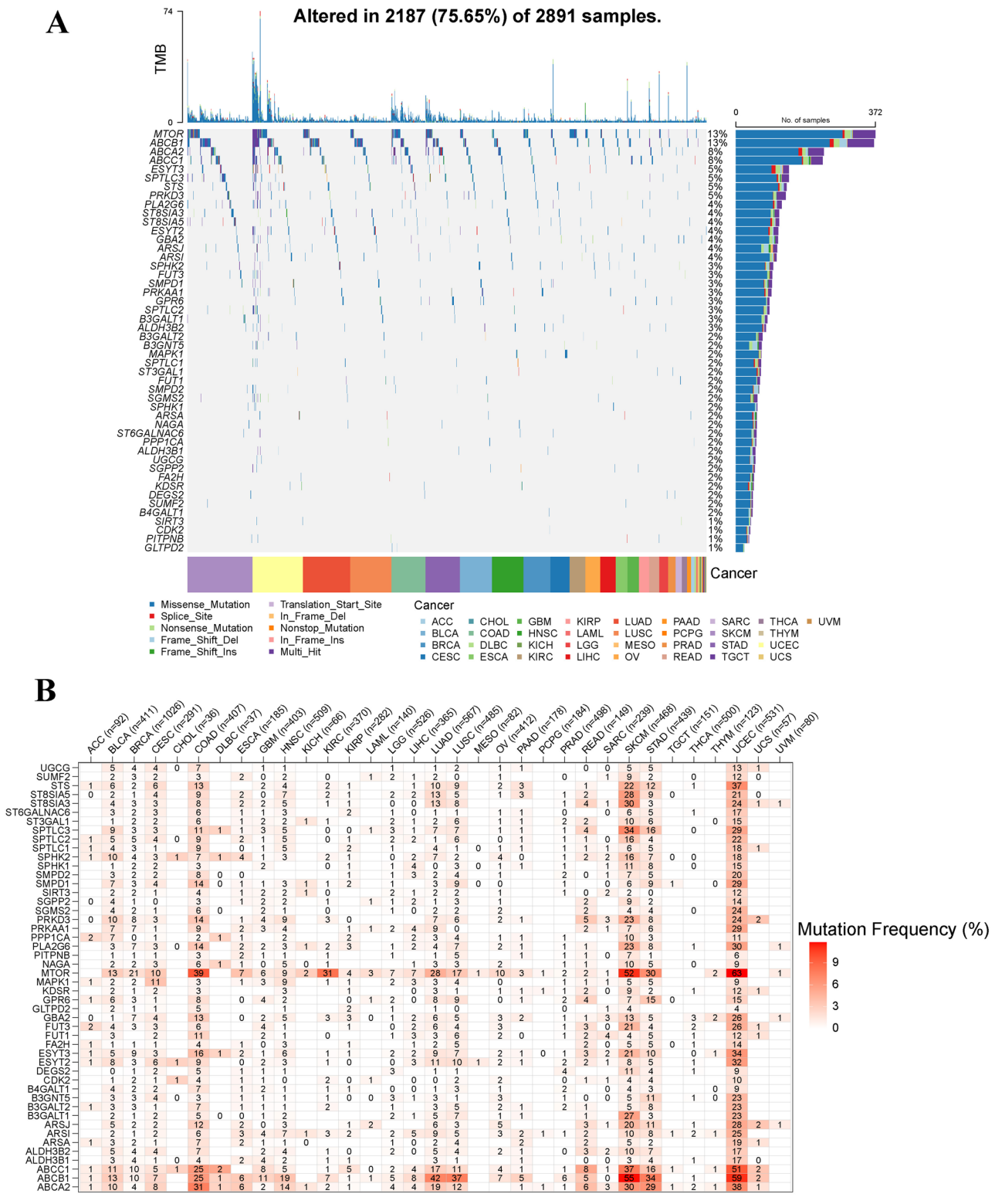

Fig. 4 Single nucleotide variation (SNV) of sphingolipid metabolism-related genes (SMRGs) in pan-cancer. **(A)** The oncoplot shows the SNV landscape of SMRGs in 33 kinds of cancers. **(B)** SNV frequency of SMRGs in 33 kinds of cancers

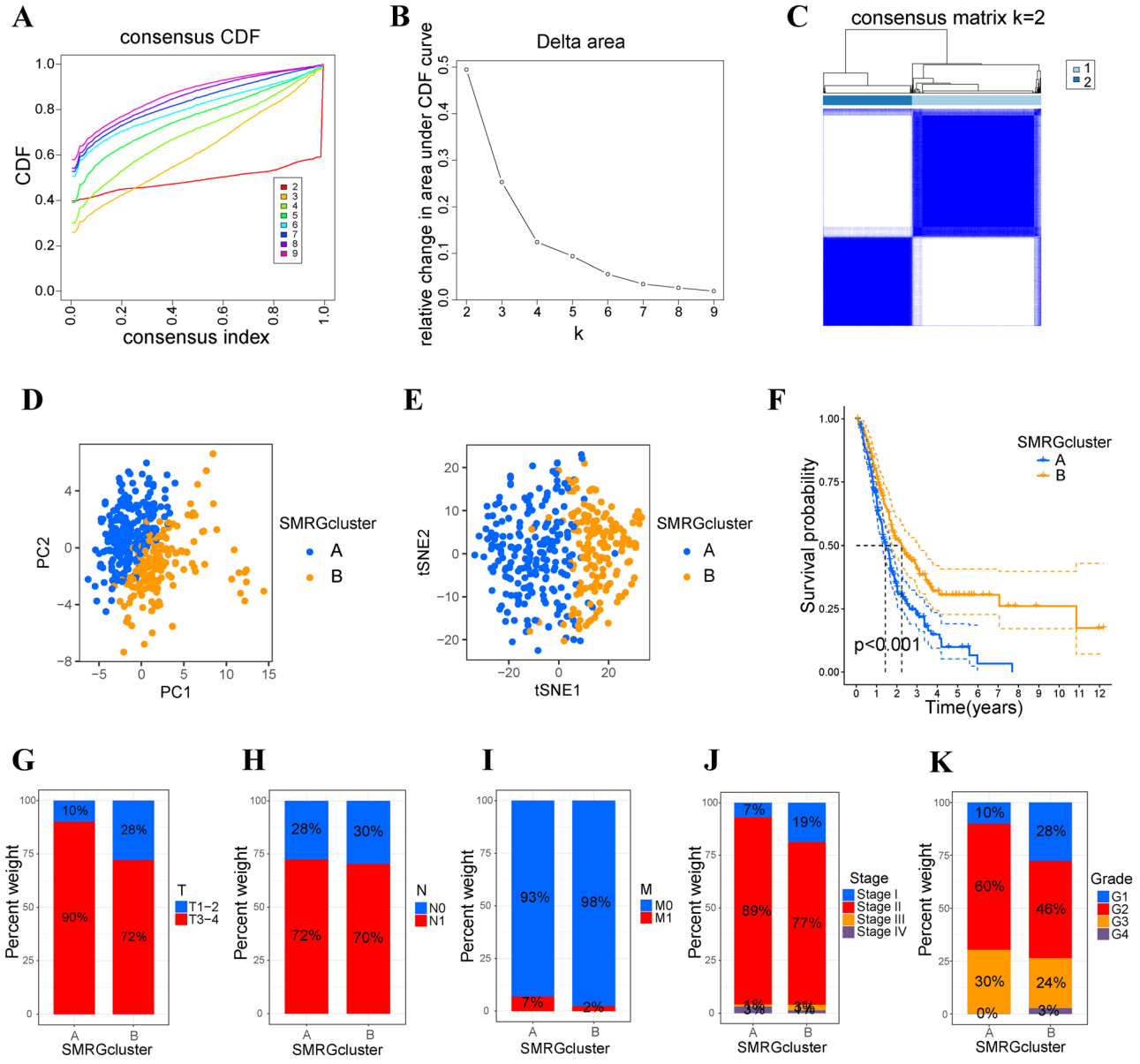

Fig. 5 Identifying the sphingolipid metabolism-related molecular subtype. **(A)** The curve for the cumulative distribution function (CDF). **(B)** The relative changes in area under the CDF curve. **(C)** Heatmap with consensus clustering. PCA **(D)** and t-SNE **(E)** could distinguish pancreatic cancer patients between SMRGcluster A and SMRGcluster B. **(F)** Survival curves of SMRGcluster A and SMRGcluster B. The proportion of the various T stages **(G)**, N stages **(H)**, M stages **(I)**, clinical stages **(J)**, and pathological grades **(K)** between SMRGcluster A and SMRGcluster B

and 122 were highly expressed in SMRGcluster B (Figure S2). GO analysis revealed that the enriched pathways for these genes included "digestion", "digestive system process", "skin development", "epidermis development", "epithelial cell proliferation", "epithelial structure maintenance", "regulation of body fluid levels", "anatomical structure homeostasis", and "regulation of epithelial cell proliferation" (Fig. 8A). KEGG analysis manifested that the enriched pathways for these genes included "pancreatic secretion", "ECM-receptor interaction", "retinol metabolism", "focal adhesion", "PI3K-Akt signaling pathway", and "glycerolipid metabolism" (Fig. 8B).

Building of SM-related prognostic model

Univariable Cox regression found that 143 SM-related DEGs were linked to the prognosis of PC (Table S3). To eliminate overfitting among genes, LASSO regression was carried out (Fig. 9A and B). Then, multivariable Cox regression was employed for building an SM-associated prognostic model, including three genes: ANLN, ANKRD22, and DKK1 (Fig. 9C). KM curves of the training set indicated that the low-risk PCs survived noticeably longer compared to the high-risk PCs (Fig. 9D), and 1-, 3-, and 5-year survival rates' AUCs were 0.773, 0.796, and 0.81, respectively (Fig. 9E). PCA as well as t-SNE may

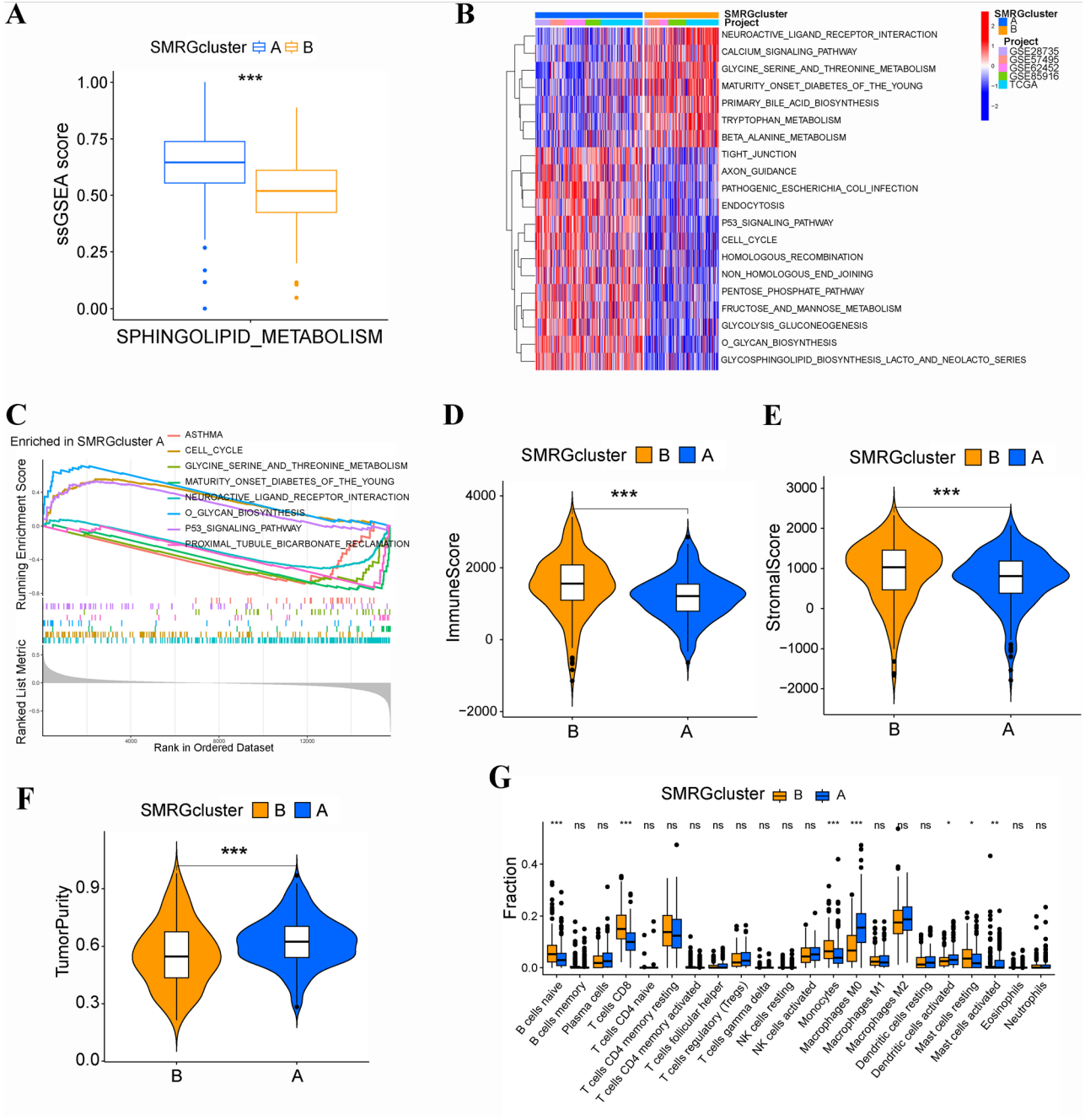

Fig. 6 ssGSEA, GSVA, GSEA, and immunoassay. **(A)** The ssGSEA score of sphingolipid metabolism between SMRGcluster A and SMRGcluster B. **(B)** GSVA. **(C)** GSEA. Immune **(D)**, stromal **(E)**, and tumour purity **(F)** scores between SMRGcluster A and SMRGcluster B. **(G)** The infiltrated levels of 22 kinds of immune cell subpopulations between SMRGcluster A and SMRGcluster B. (ns denotes not significant; * denotes $p < 0.05$; ** denotes $p < 0.01$; *** denotes $p < 0.001$)

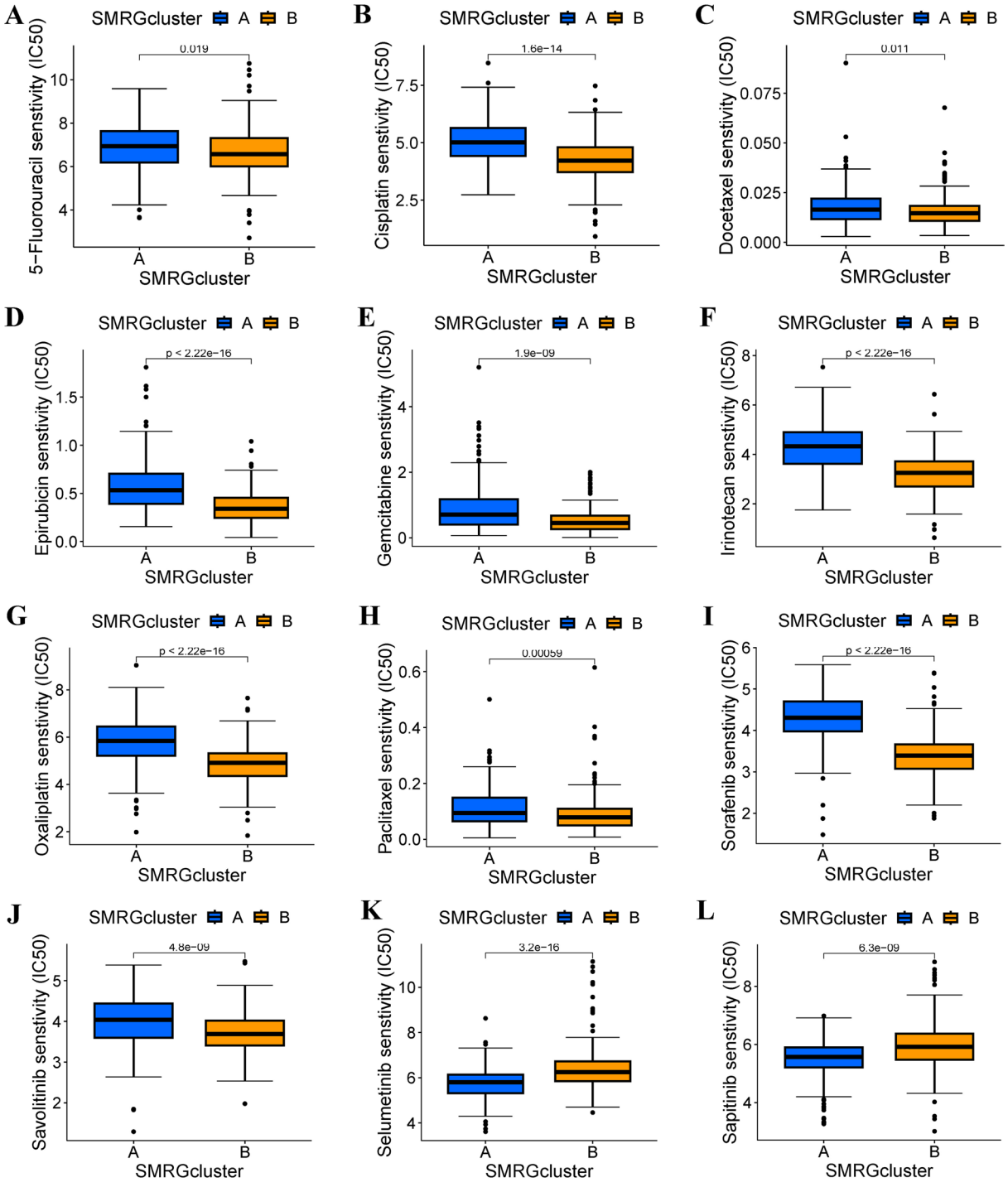

Fig. 7 Drug sensitivity between different subtypes. SMRGcluster B was more sensitive to 5-fluorouracil **(A)**, cisplatin **(B)**, docetaxel **(C)**, epirubicin **(D)**, gemcitabine **(E)**, irinotecan **(F)**, oxaliplatin **(G)**, paclitaxel **(H)**, sorafenib **(I)**, and savolitinib **(J)**. SMRGcluster A was more sensitive to selumetinib **(K)** and sapitinib **(L)**

accurately identify PCs with various risks (Fig. 9F). Additionally, the internal (Fig. 9G) and external (Fig. 9J) validation sets also indicated that the low-risk PCs survived noticeably longer compared to the high-risk PCs. The 1-, 3-, and 5-year survival rates' AUCs were 0.691, 0.763, and 0.760 in the internal validation set (Fig. 9H), and 0.622, 0.634, and 0.667 in the external validation set (Fig. 9K). PCA and t-SNE could also clearly distinguish samples between different risk groups within the internal (Fig. 9I) and external (Fig. 9L) validation sets.

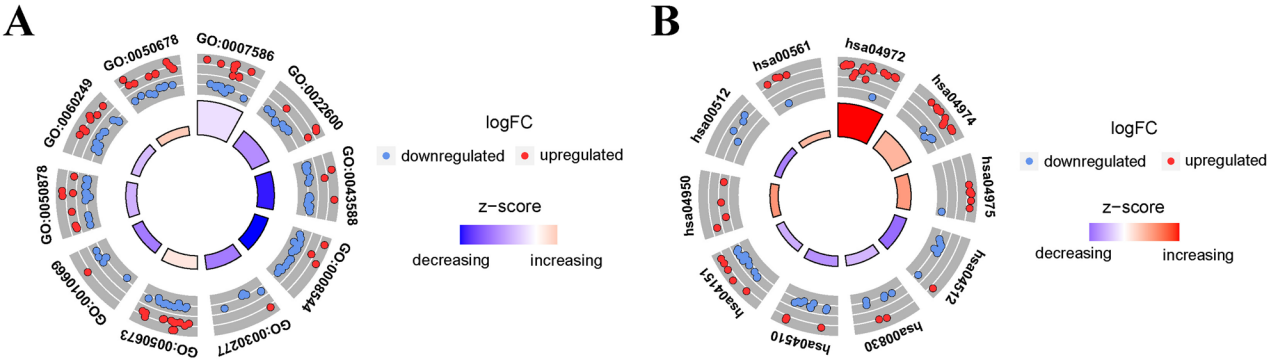

ID	Description
GO:0007586	digestion
GO:0022600	digestive system process
GO:0043588	skin development
GO:0008544	epidermis development
GO:0030277	maintenance of gastrointestinal epithelium
GO:0050673	epithelial cell proliferation
GO:0010669	epithelial structure maintenance
GO:0050878	regulation of body fluid levels
GO:0060249	anatomical structure homeostasis
GO:0050678	regulation of epithelial cell proliferation

ID	Description
hsa04972	Pancreatic secretion
hsa04974	Protein digestion and absorption
hsa04975	Fat digestion and absorption
hsa04512	ECM−receptor interaction
hsa00830	Retinol metabolism
hsa04510	Focal adhesion
hsa04151	PI3K−Akt signaling pathway
hsa04950	Maturity onset diabetes of the young
hsa00512	Mucin type O−glycan biosynthesis
hsa00561	Glycerolipid metabolism

Fig. 8 Enrichment analysis. **(A)** Gene Ontology enrichment analysis. **(B)** Kyoto Encyclopedia of Genes and Genomes enrichment analysis

Relationship of SM-related risk score with clinicopathological features and immune microenvironment

PCs with T3-4 stages had a significantly higher risk score than those with T1-2 stages (Fig. 10A). The risk scores were higher in PCs with a higher clinical stage or pathological grade (Fig. 10B and C). PCs with N1 and M1 stages had higher risk scores than those with the corresponding N0 and M0 stages, but the difference was not statistically significant (Figure S3 and Figure S4). Multivariable Cox regression analysis indicated that SM-related risk score is an independent risk factor for PC, regardless of clinicopathological characteristics (Figure S5). Correlation analysis manifested risk score was significantly positively correlated with SM score (Fig. 10D). ANKRD22, ANLN, and DKK1 also showed a significant positive correlation with SM score, among which ANKRD22 had the most significant correlation (Fig. 10E-G). Immune analysis manifested that the infiltrated abundance of naïve B cells, CD8+T cells, resting memory CD4+T cells, monocytes, and resting mast cells were higher in low-risk PC, but follicular helper T cells, M0 and M1 macrophages, active DCs, active mast cells, and neutrophils had higher infiltrated abundance in high-risk PC (Fig. 10H). Further correlation analysis manifested that SM score, risk score, ANKRD22, ANLN, and DKK1 were significantly positively correlated with M0 macrophages, but negatively correlated with monocytes (Fig. 10I).

Drug sensitivity in high- and low-risk groups

Evaluating the sensitivity of each patient to various drug treatments is necessary and can help clinicians reasonably formulate individualized therapy regimens for PC patients. This study discovered that the low-risk PCs were more sensitive to cisplatin, epirubicin, fludarabine, gemcitabine, irinotecan, oxaliplatin, and sorafenib (Fig. 11A-G). While the high-risk PCs were more sensitive to selumetinib and ulixertinib (Fig. 11H and I).

Expression of model genes

The RNA-expressed levels of ANLN, ANKRD22, and DKK1 were investigated via GSE28735 and GSE62452 datasets. Results showed that ANKRD22, ANLN, and DKK1 had higher RNA expression levels in PC tissues than in normal tissues (Fig. 12A-B). Proteomic data from CPTAC database suggested that ANKRD22, ANLN, and DKK1 had higher protein levels in PC tissues (Fig. 12C-E). The immunohistochemistry images of ANLN and ANKRD22 were also downloaded via HPA platform. Immunohistochemistry images showed that ANLN and ANKRD22 had stronger protein expression in PC tissues than in adjacent tissues (Fig. 12F and G). To illustrate the dependability of these findings, the expression of ANLN, ANKRD22, and DKK1 was verified using PCR. Results suggested that the expression of ANLN, ANKRD22, and DKK1 was higher in PC cells compared to pancreatic ductal epithelial cells (Fig. 12H-J).

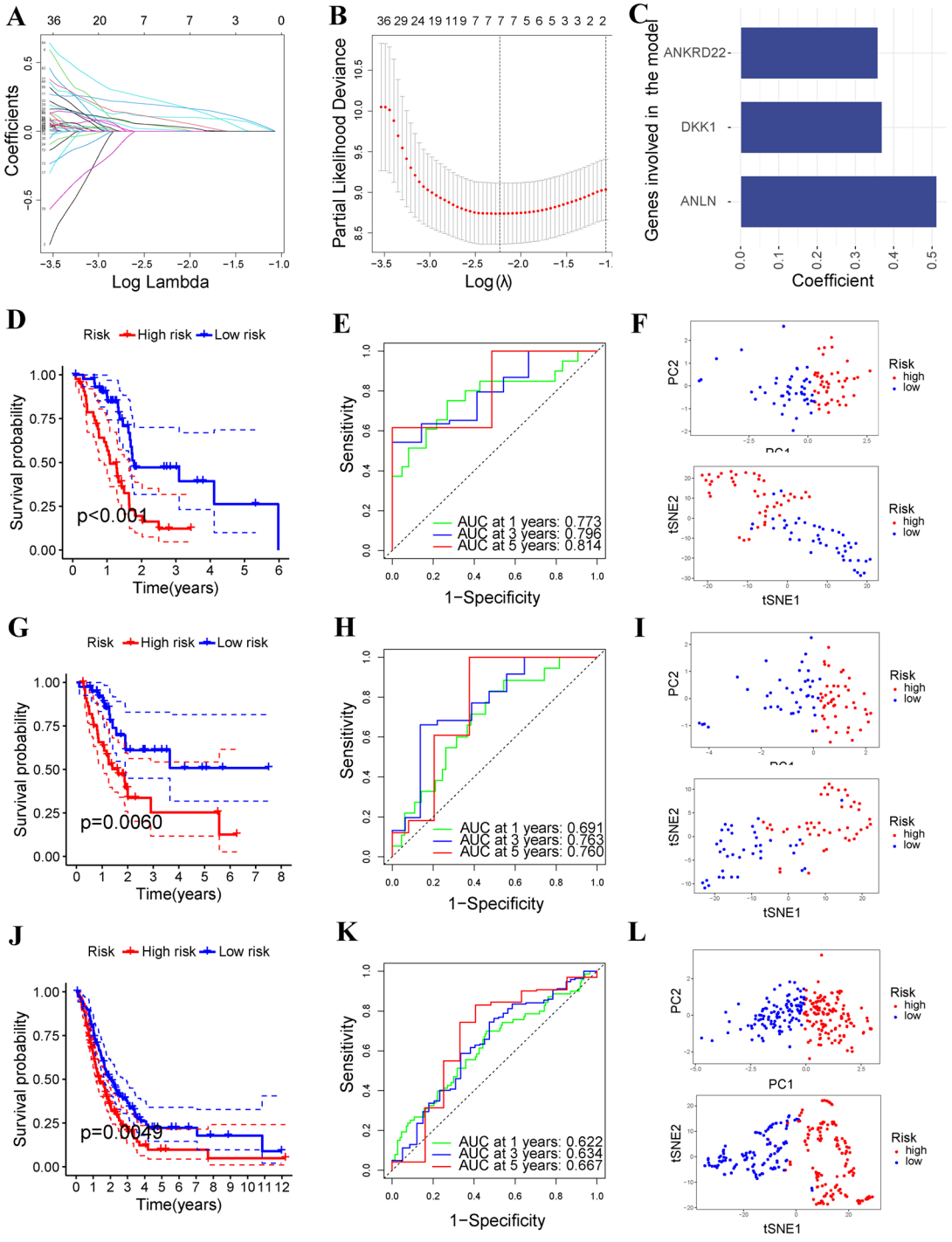

Fig. 9 Construction and validation of sphingolipid metabolism-related prognostic model. **(A)** Coefficient path diagram. **(B)** Cross-validation curve. **(C)** Coefficients of genes in the model. Survival curve **(D)**, ROC curve **(E)**, and PCA and t-SNE **(F)** in the training cohort. Survival curve **(G)**, ROC curve **(H)**, and PCA and t-SNE **(I)** in the internal validation cohort. Survival curve **(J)**, ROC curve **(K)**, PCA and t-SNE **(L)** in the external validation cohort

PPI and ceRNA networks

For exploring which proteins interact with ANLN, ANKRD22, and DKK1, PPI networks were constructed. Results showed that ANKRD22 interacts with POTED, BATF2, ETV7, FCGR1B, GBP5, STAMBPL1, POTEM, LOC100288966, SLC25A45, ANKRD1, and these proteins may be involved in relevant biological processes together (Fig. 13A). ANLN interacts with BUB1, CEP55, DIAPH3, ECT2, KIF11, KIF20A, KIF23, RACGAP1, TPX2, and RHOA (Fig. 13B). DKK1 interacts with

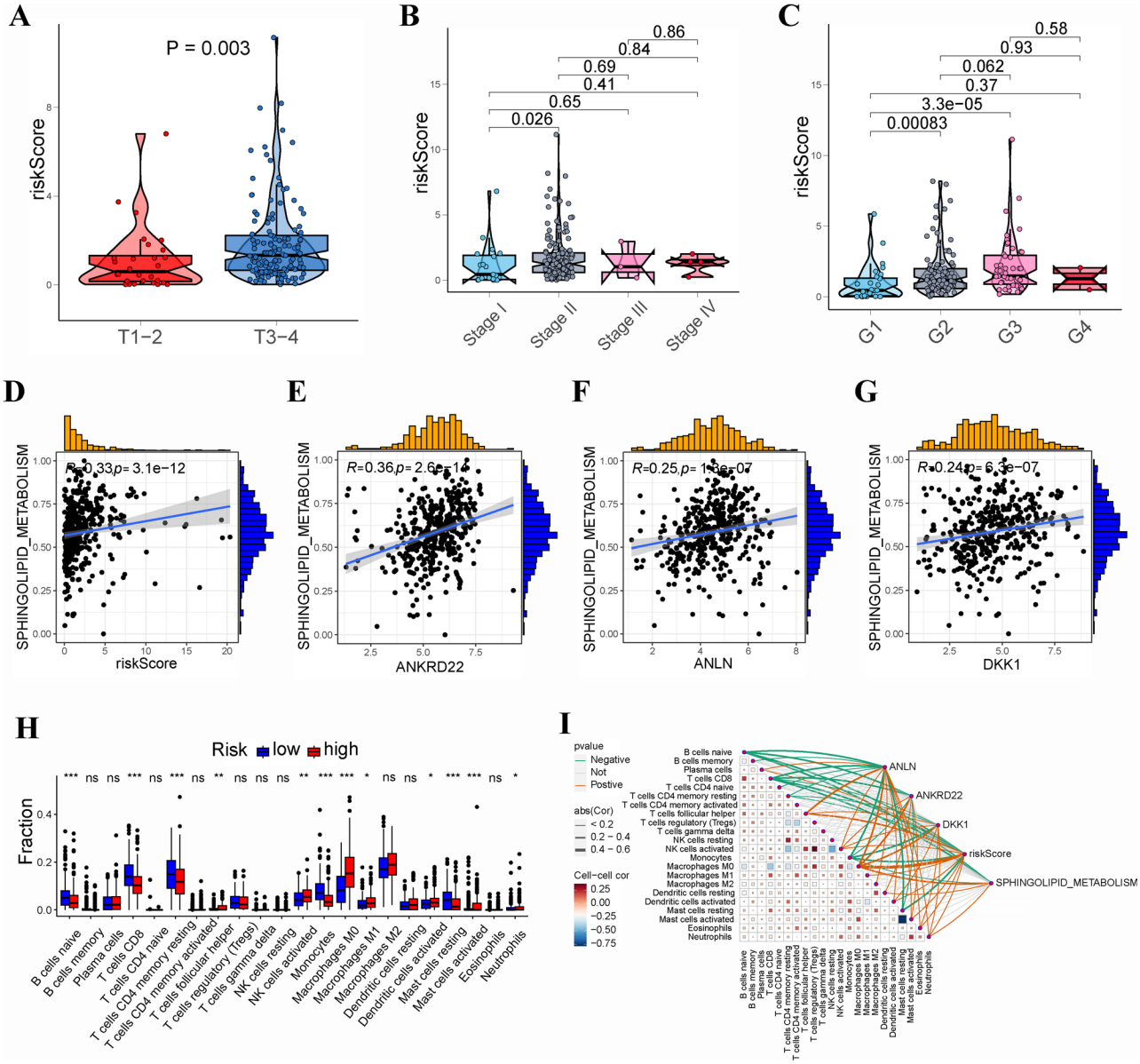

Fig. 10 Relationship of sphingolipid metabolism-related risk score with clinicopathological features and immune microenvironment. **(A)** PC with T3-4 stages had a higher risk score compared to PC with T1-2 stages. **(B)** PC with high clinical stages had a higher risk score compared to PC with low clinical stages. **(C)** PC with a high pathological grade had a higher risk score compared PC with a low pathological grade. Correlation of sphingolipid metabolism with risk score **(D)**, ANKRD22 **(E)**, ANLN **(F)**, and DKK1 **(G)**. **(H)** The infiltrated abundance of immune cell subpopulations between high- and low-risk PC. **(I)** Correlation of immune cell subpopulations, risk score, ANKRD22, ANLN, and DKK1. (ns denotes not significant; * denotes $p < 0.05$; ** denotes $p < 0.01$; *** denotes $p < 0.001$)

CKAP4, CTNNB1, DKK3, KREMEN1, KREMEN2, LRP5, LRP6, SOST, WNT1, and WNT3A (Fig. 13C). In addition, ceRNA networks were built to investigate the regulatory mechanisms of ANLN, ANKRD22, and DKK1. The ceRNA networks included 63 nodes (3 mRNA, 11 miRNA, and 49 lncRNA) and 64 edges (Fig. 13D).

Single-cell analysis

A total of 3 PC samples containing 29,294 cells were collected from GSE214295 dataset. And 22,935 cells were obtained after the quality control (Figure S6). After dimensionality reduction and clustering, the cells of 3 PC samples were shown in Fig. 14A. A total of 26 cell clusters were identified (Fig. 14B). After cell annotation, 10 cell subpopulations were identified, including B cells, CMP, endothelial cells, epithelial cells, macrophages, neurons, neutrophils, smooth muscle cells, T cells, and tissue stem cells (Fig. 14C). Epithelial cells, tissue stem cells, and macrophages had more abundant intercellular communication (Fig. 14D). ANKRD22, DKK1, and ANLN have

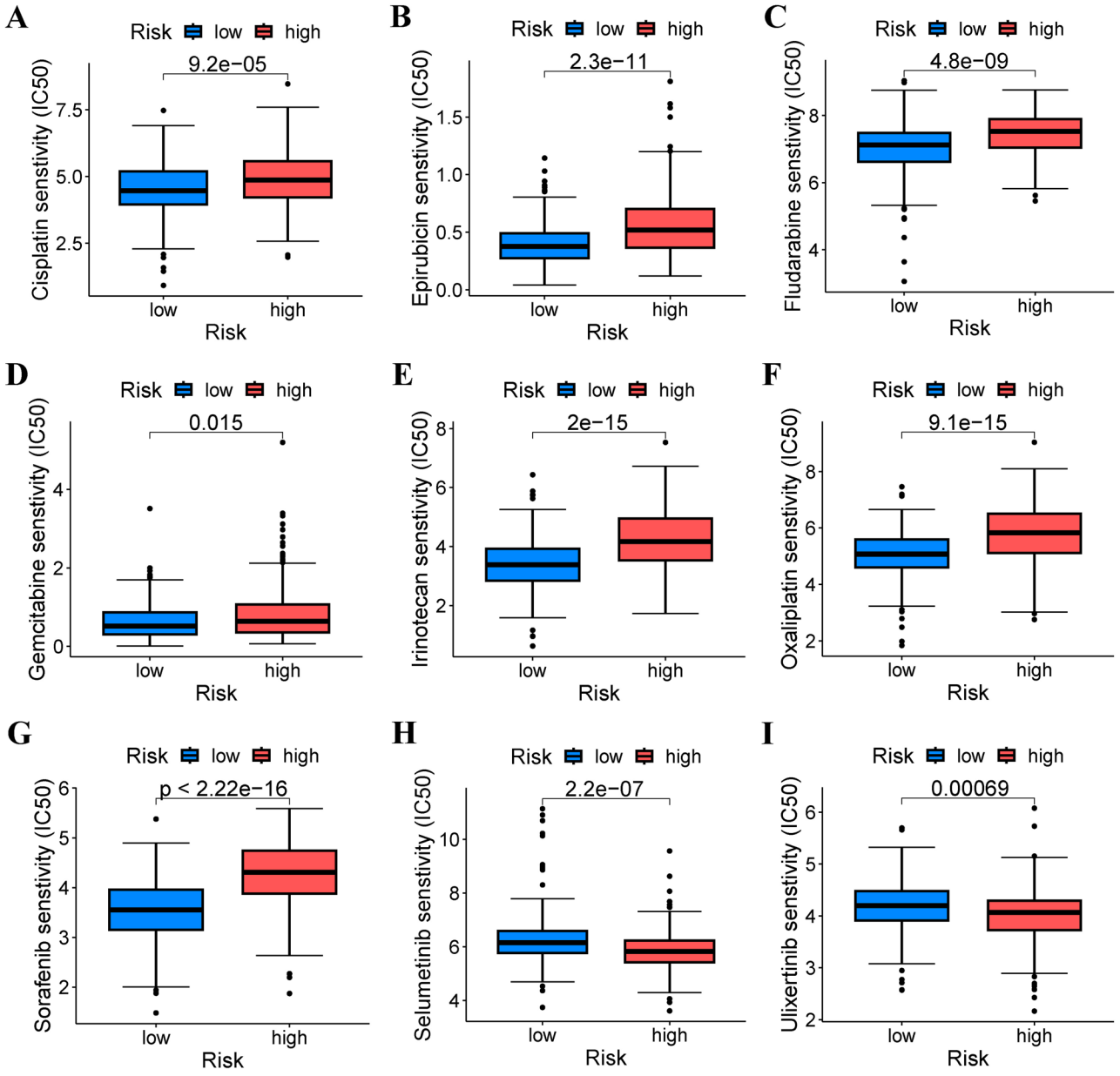

Fig. 11 Drug sensitivity between different risk groups. The low-risk PC had higher sensitivity to cisplatin **(A)**, epirubicin **(B)**, fludarabine **(C)**, gemcitabine **(D)**, irinotecan **(E)**, oxaliplatin **(F)**, and sorafenib **(G)**. The high-risk PC had higher sensitivity to selumetinib **(H)** and ulixertinib **(I)**

high expression levels in epithelial cells (Fig. 14E-G). Then, the SM score was evaluated in each cell subpopulation using "UCell", "singscore", and "AddModuleScore" algorithms, and the results showed that macrophages, epithelial cells, and endothelial cells had relatively high SM scores (Fig. 14H). According to the expression levels of ANKRD22, DKK1, and ANLN, each cell subpopulation was divided into high- or low-expression groups. The results showed that epithelial cells, tissue stem cells, and macrophages with ANKRD22 high expression had more active SM, and interestingly, B cells with ANKRD22 low expression had more active SM (Fig. 14I). Epithelial cells and tissue stem cells with DKK1 high expression had more active SM (Fig. 14J). Epithelial cells, tissue stem cells, and B cells with ANLN high expression had more active SM (Fig. 14K).

ANKRD22 knockdown could restrain the proliferation, migration, and invasion of PC cells

By reviewing the published literature, ANLN and DKK1 knockdown have been shown to inhibit the proliferation and aggressiveness of PC cells. However, the function of ANKRD22 in PC cells has not been reported. Therefore, in vitro experiments were conducted to investigate the

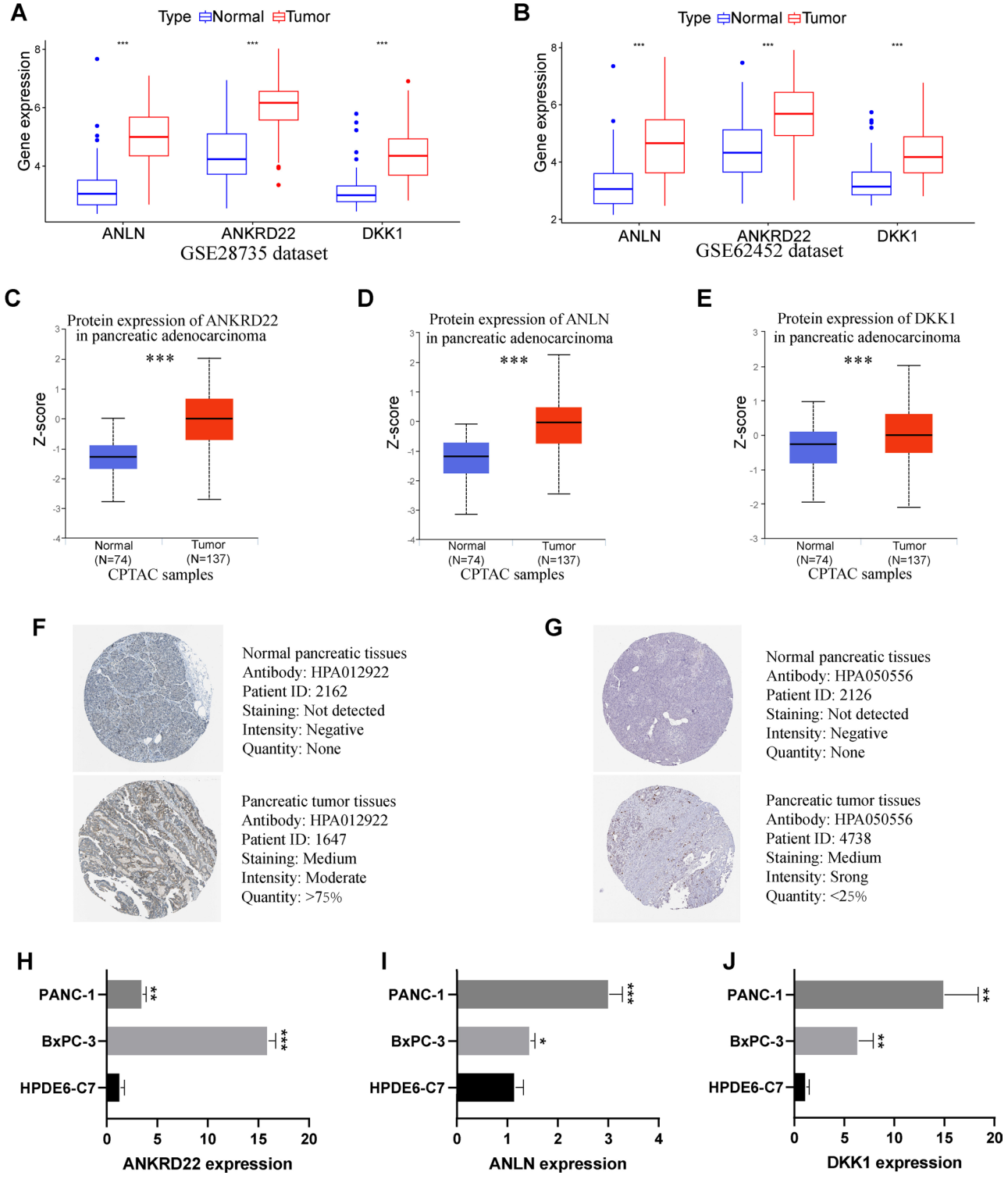

Fig. 12 Expression of model genes. GSE28735 **(A)** and GSE62452 **(B)** datasets showed that the RNA expression of ANKRD22, ANLN, and DKK1 was higher in pancreatic tumour tissues than normal tissues. The protein expression of ANKRD22 **(C)**, ANLN **(D)**, and DKK1 **(E)** was higher in pancreatic tumour tissues. Immunohistochemical image of ANKRD22 **(F)** and ANLN **(G)** in pancreatic tumour. In comparison to pancreatic ductal epithelial cells, pancreatic cancer cell lines express ANKRD22 **(H)**, ANLN **(I)**, and DKK1 **(J)** at relatively higher levels. (ns denotes not significant; * denotes $p < 0.05$; ** denotes $p < 0.01$; *** denotes $p < 0.001$)

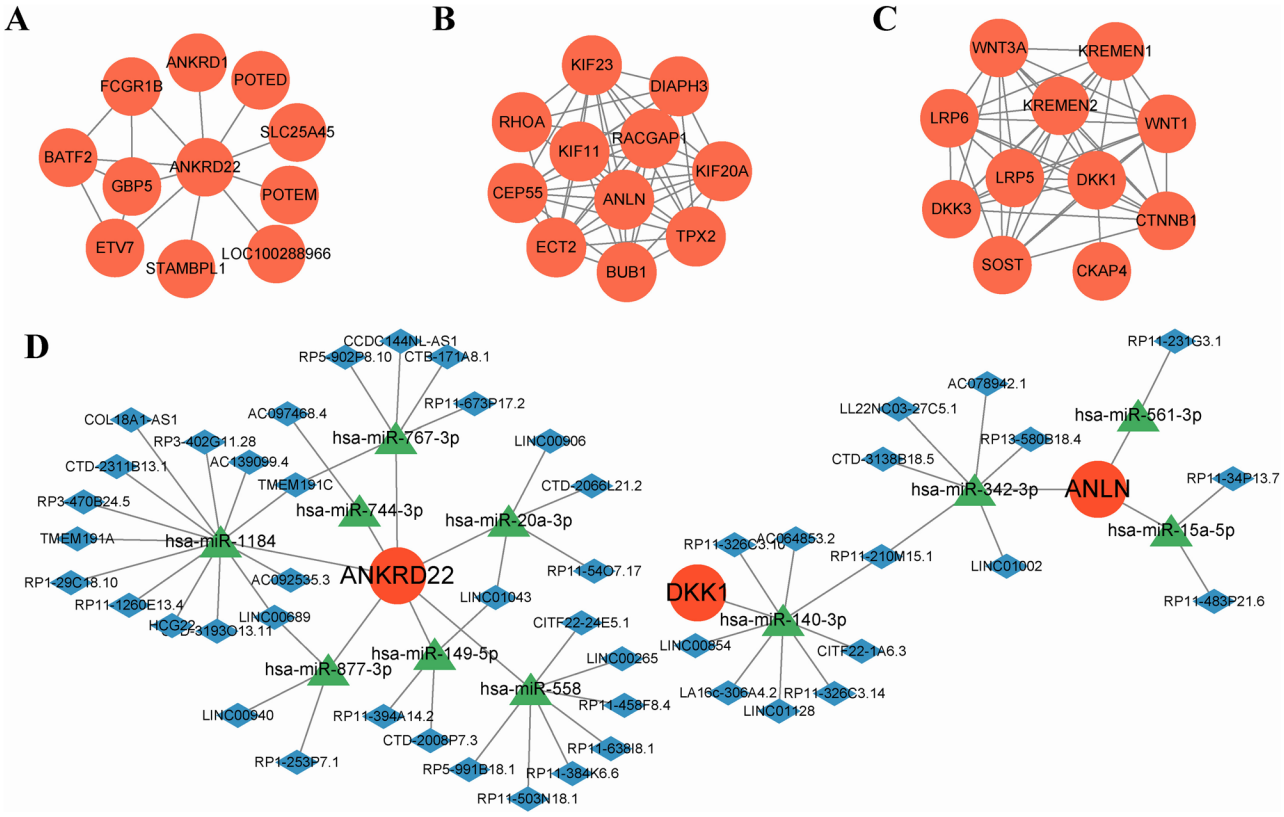

Fig. 13 Protein–protein interaction (PPI) and competitive endogenous RNA (ceRNA) networks. PPI networks were constructed using ANKRD22 **(A)**, ANLN **(B)**, and DKK1 **(C)**. **(D)** The ceRNA included 63 nodes and 64 edges (Circle represents mRNA, triangle represents miRNA, and diamond represents lncRNA)

function of ANKRD22 in PC cells. The siRNA targeting ANKRD22 was transfected into PC cells BxPC-3 and PANC-1. PCR results confirmed the successful knockdown of ANKRD22 expression (Fig. 15A and B). CCK-8 assays demonstrated that the knockdown of ANKRD22 inhibited the growth of BxPC-3 and PANC-1 cells (Fig. 15C and D). Scratch assays revealed that the knockdown of ANKRD22 significantly reduced the migration of BxPC-3 and PANC-1 cells (Fig. 15E and F). Transwell invasion assays indicated that the knockdown of ANKRD22 effectively inhibited the invasion of PANC-1 and BxPC-3 cells (Fig. 15G and H). Based on the above results, it can be concluded that ANKRD22 knockdown can inhibit the proliferation, migration, and invasion of PC cells, which can be used as a potential therapeutic strategy for PC.

Discussion

PC is a highly malignant tumour that progresses quickly and has a terrible outcome [47]. Effective diagnosis and treatment of PC have always been challenges for clinicians [48]. Currently, radical surgery remains the only possible cure for PC. Although the multi-strategy diagnosis and treatment of malignant tumours have been continuously improved in recent years, PC tumour microenvironment is diverse and heterogeneous, which makes adjuvant therapy low sensitive. Therefore, the prognosis of PC is worse than that of other gastrointestinal tumours [49]. Recently, the role of SM in tumour pathogenesis has attracted more and more researchers' attention [50]. Studies found that abnormal SM played important functions in tumour cell survival, growth, invasion, and treatment resistance [51, 52]. The quick progress of high-throughput sequencing technology and microarrays running on high-throughput platforms provides new strategies for screening latent targets for cancer diagnosis and therapy [53–56]. Multi-omics techniques have also been widely used in cancer research [57–59]. This study utilized bulk and single-cell profiling to characterize SM in PC, which provided a new perspective for patient stratification and precision medicine of PC.

SM is a highly complex process, and its imbalance can lead to the occurrence, development, and metastasis of tumours by activating or inhibiting cell signal transduction [60]. Malavaud et al. [61] found that SPHK1 in prostate cancer tissues was upregulated and may be a potential biomarker for diagnosis. Increased expression of sphingolipid metabolism-related genes has also been found in breast, esophageal, gastric, hepatocellular, and

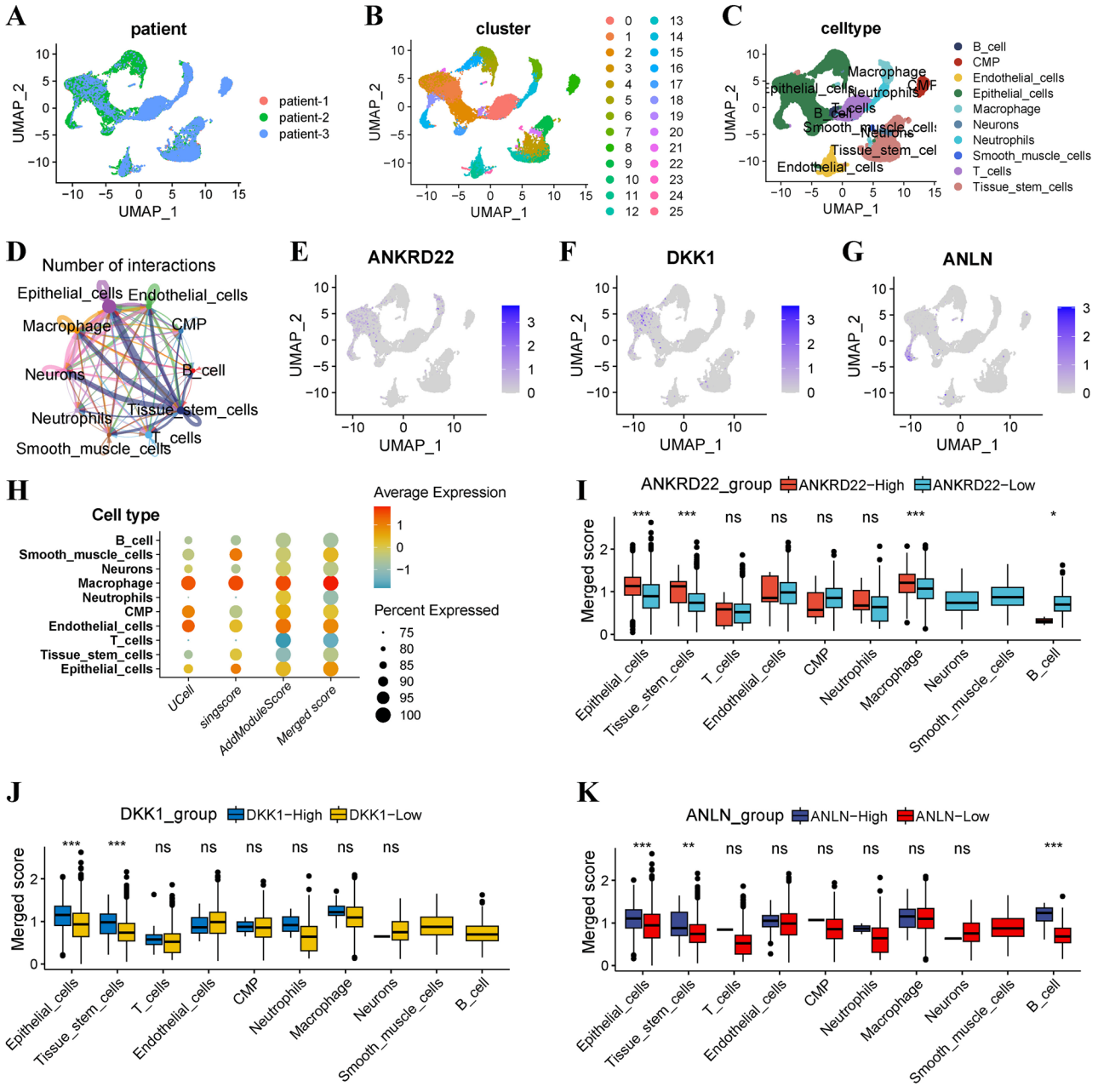

Fig. 14 Single-cell analysis. **(A)** UMAP plot showed the distribution of cells in various samples. **(B)** UMAP plot showed that a total of 26 cell clusters were identified. **(C)** UMAP plot showed that 10 cell subpopulations were identified. **(D)** Intercellular communication. UMAP plot showed that the expression distribution of ANKRD22 **(E)**, DKK1 **(F)**, and ANLN **(G)**. **(H)** The score of sphingolipid metabolism in each cell subpopulation was assessed by "UCell", "singscore", and "AddModuleScore" algorithms. Epithelial cells and tissue stem cells with high expression of ANKRD22 **(I)**, DKK1 **(J)**, and ANLN **(K)** had more active sphingolipid metabolism activity. (ns denotes not significant; * denotes $p < 0.05$; ** denotes $p < 0.01$; *** denotes $p < 0.001$)

ovarian cancers [62–65]. This study suggested that most SMRGs were related to PC prognosis, and PCA and t-SNE based on the expression of SMRGs can clearly distinguish PC tissues from normal tissues. These results revealed that SMRGs were involved in the occurrence of PC and could be used as candidate markers for PC diagnosis and therapy. Hu et al. [66] found that the abnormal activity of SM was related to the distant metastasis of osteosarcoma, which could offer a fresh strategy for the treatment of osteosarcoma. A meta-analysis [67] showed that abnormally elevated expression of SPHK1 was linked to poor prognosis in cancer patients. Two SM-associated molecular subtypes (SMRGcluster A and SMRGcluster B) were identified in this study. PCs in SMRGcluster A had a more advanced clinical stage, worse pathological grade, and shorter survival. The ssGSEA analysis further

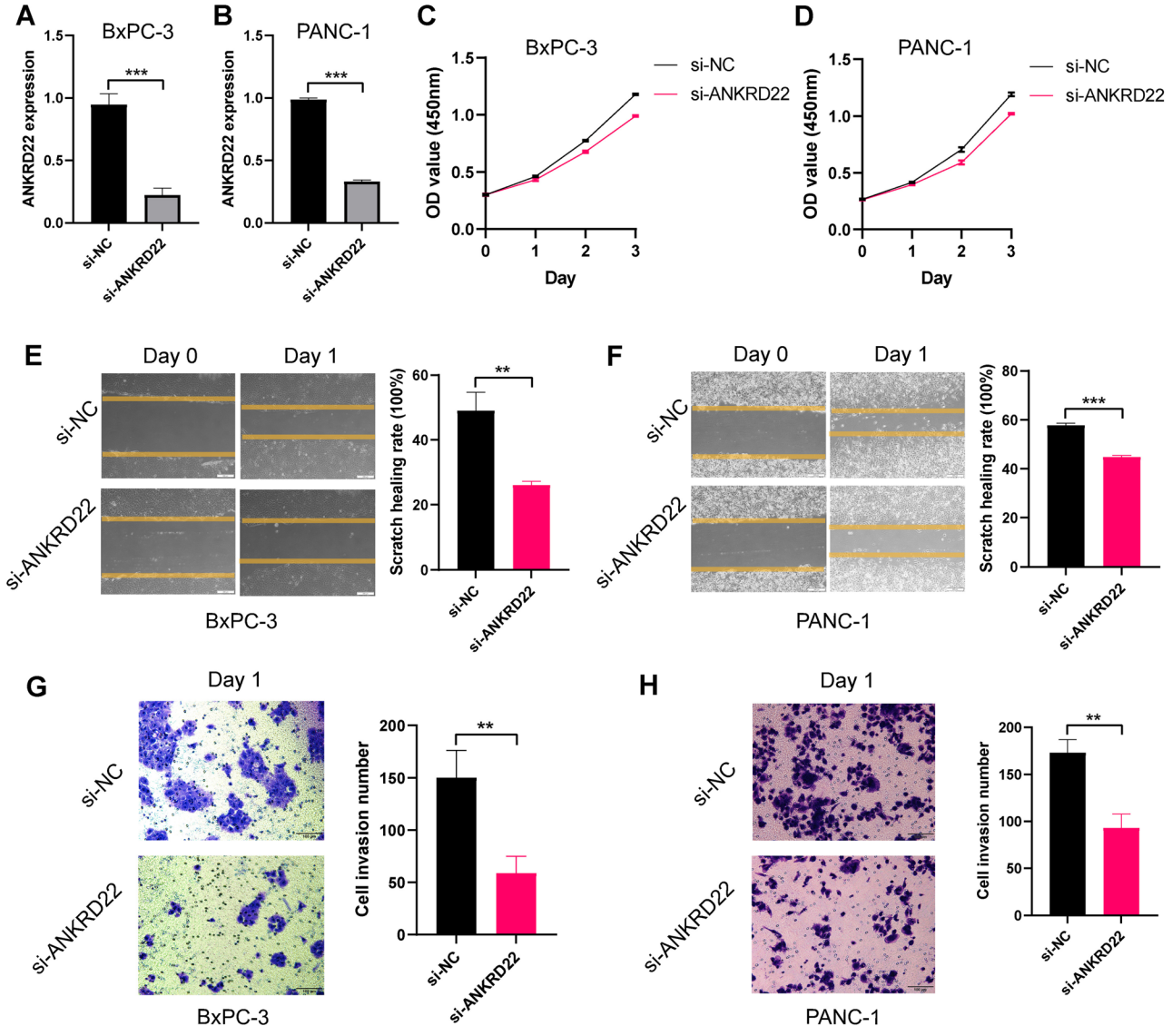

Fig. 15 In vitro experiment. PCR showed that the expression of ANKRD22 was knocked down in BxPC-3 cells **(A)** and PANC-1 cells **(B)**. CCK-8 assays indicated that ANKRD22 knockdown could inhibit the proliferation of BxPC-3 cells **(C)** and PANC-1 cells **(D)**. Scratch assays indicated that ANKRD22 knockdown could inhibit the migration of BxPC-3 cells **(E)** and PANC-1 cells **(F)**. Transwell invasion assays indicated that ANKRD22 knockdown could inhibit the invasion of BxPC-3 cells **(G)** and PANC-1 cells **(H)**. (ns denotes not significant; * denotes $p < 0.05$; ** denotes $p < 0.01$; *** denotes $p < 0.001$)

revealed that SMRGcluster A had a more active SM process.

Tumour microenvironment is a hot topic in oncology research [68–70]. Besides tumour cells, tumour microenvironment also contains immune cells, stromal cells, and stromal components that are connected to tumour occurrence and development [71, 72]. Sphingolipid is an important component of cell membrane, and their abnormal metabolism will affect the activity of immune cell surface receptors, thereby interfering with immune response of tumour cells [71]. Weigert et al. [73] showed that tumour cell apoptosis-derived S1P could contribute to M2 phenotypic transition of macrophages in tumour microenvironment. In this study, single-cell analysis was implemented to reveal that SM had higher scores in macrophage. Studies by Nema et al. [74] found that sphingosine-1-phosphate or lipid-phosphatase-3 was connected with the infiltrations of CD8+T cells, neutrophils, and macrophages. CD8+T cells can recognize tumour cell surface antigens and kill tumour cells, and their high infiltration is considered to be connected with a good outcome [75]. The function of B cells within tumour microenvironment is complex and controversial, which may be related to different subsets and functional states of B cells [76, 77]. On the one hand, B cells have the function of antigen presentation, eliciting immune responses

against tumours, and enhancing the prognosis for cancer patients [78, 79]. However, some studies have also shown that B cells are linked to tumour progression and poor prognosis. For example, the degree of tumour angiogenesis is linked to the existence of B cells with STAT3 activity, indicating that these cells are regulators of tumour development and possible targets for treatment [80]. CD19+B cells were linked to metastasis and poorer outcome of ovarian cancer [81]. The connection between SM-associated molecular subtype and tumour microenvironment was evaluated using the "ESTIMATE" and "CIBERSORT" algorithms in this study. The infiltrated levels of naïve B cells and CD8+T cells were higher in SMRGcluster B with a better prognosis, while the infiltrated levels of macrophage M0 and activated dendritic cells were higher in SMRGcluster A with a poorer prognosis.

Primary and secondary drug resistance is a great challenge for cancer therapy [82]. It is of great significance to clarify the sensitivity of each patient to specific drug treatment and improve the response to drug treatment to improve drug efficacy and formulate individualized treatment plans [83]. Many studies have shown that abnormal SM can affect drug sensitivity. Li et al. [84] revealed that enoyl-CoA hydratase could induce colorectal cancer cell resistance to 5-fluorouracil and oxaliplatin by promoting UDP-glucose ceramide glycosyltransferase-mediated glycosylation of ceramide glycosylation. The study by Wang et al. [85] demonstrated that hepatocellular carcinoma had abnormally high levels of SPHK1 expression, which was linked to a poor outcome and oxaliplatin resistance. This study suggested that PC patients in SMRGcluster B had higher sensitivity to 5-fluorouracil, docetaxel, epirubicin, gemcitabine, oxaliplatin, paclitaxel, savolitinib, and sorafenib. Therefore, exploring the mechanism of abnormal SM in patients with PC may provide a new strategy for clarifying drug sensitivity and contributing to realizing scientifically individualized treatment.

To accurately assess the prognosis of each PC patient, an SM-related prognostic model (including three genes ANKRD22, ANLN, and DKK1) was built in this study. ANKRD22 was found to be a mitochondrial protein that can interact with multiple subunits of phosphoinositide-dependent kinase-1 and ATP synthase complex, involved in metabolic reprogramming [86, 87]. Pan et al. [87] found that ANKRD22 and extended synaptopagmin-1 worked together to transfer extra lipids into mitochondria and decrease the number of mitochondria, which promoted metabolism reprogramming in colon cancer cells. Wu et al. [88] showed that breast cancer patients had abnormally high levels of ANKRD22 expression, which triggered the Wnt/-catenin signaling pathway by controlling NUSAP1 and encouraged breast cancer metastasis. Yin et al. [89] found that ANKRD22 was connected with a bad outcome and recurrence of lung cancer. This research indicated that the expression of ANKRD22 was up-regulated within PC tissues and linked to a bad outcome. Moreover, single-cell analysis suggested that ANKRD22 was associated with a high score of SM in macrophage, which may promote tumour development by influencing SM process of macrophage. ANLN can encode Anlin protein, a ubiquitously expressed actin-binding protein, which can regulate tumour cell migration. ANLN expression is elevated in numerous malignant tumours and is linked to bad outcome [90, 91]. This study suggested that ANLN was linked to the bad outcome in PC and could be a possible therapeutic target. DKK1, a member of the Dickkopf family, may prevent LRP5/6 interaction with Wnt, hence preventing β-catenin-dependent Wnt signaling pathway [92]. The influence of DKK1 on malignant tumours is still controversial. The study by Hall et al. [93] revealed that DKK1 expression was elevated in early prostate cancer. However, with the disease progression, especially advanced bone metastasis, the expressed level of DKK1 decreased. Betella et al. [94] found that the overexpression of DKK1 was linked to the suppressed immune microenvironment, and could be a latent therapy target of ovarian cancer. In vivo experiments revealed that DKK1 could interact with cytoskeleton-associated protein 4 on the surface of macrophages, then activate downstream PI3K-AKT signaling and promote immune suppression [95]. This study indicated that DKK1 expression was increased within PC and was linked to a bad prognosis.

This study identified SM-associated molecular subtype and prognostic model for PC, and comprehensively assessed the prognosis, clinicopathological features, tumour microenvironment, and therapy response in various molecular subtypes and risk subgroups. However, this study has several shortcomings as well. First, PC samples were obtained through public databases, and the prospective clinical cohort remains indispensable to verifying the dependability of the SM-related prognostic model. Second, the molecular mechanisms of ANKRD22, ANLN, and DKK1 in PC development and prognosis still need to be explored by more in-depth experiments in future studies.

Conclusion

This study identified SM-associated molecular subtypes and prognostic model in PC, which revealed abnormal SM was related to the development, prognosis, immune microenvironment, and therapy responses of PC. Single-cell analysis revealed that SM had a relatively higher level in macrophages, epithelial cells, and endothelial cells in PC microenvironment. Cell subpopulations with high expression of ANKRD22, DKK1, and ANLN had more active SM. ANKRD22 knockdown can inhibit the proliferation, migration, and invasion of PC cells. These results

offer novel perspectives and strategies on the stratification, prognostic prediction, and precision treatment of PC patients.

Abbreviations

PC	Pancreatic cancer
S1P	sphingosine-1-phosphate
SM	sphingolipid metabolism
SPHK	sphingosine kinase
SMRGs	SM-related genes
TCGA	The Cancer Genome Atlas
GEO	Gene Expression Omnibus
MSigDB	Molecular Signatures Database
CNV	Copy number variation
CDF	cumulative distribution function
PCA	principal component analysis
t-SNE	t-distributed stochastic neighbour embedding
ssGSEA	Single-sample gene set enrichment analysis
GSVA	gene set variation analysis
IC50	half maximal inhibitory concentration
DEGs	differentially expressed genes
GO	Gene Ontology
KEGG	Kyoto Encyclopedia of Genes and Genomes
KM	Kaplan-Meier
ROC	receiver operating characteristic
AUC	area under the curve
HPA	Human Protein Atlas
scRNA	Single-cell RNA

Supplementary Information

The online version contains supplementary material available at https://doi.org/10.1186/s12885-024-13114-8.

Supplementary Material 1

Supplementary Material 2

Supplementary Material 3

Supplementary Material 4

Supplementary Material 5

Supplementary Material 6

Supplementary Material 7

Supplementary Material 8

Supplementary Material 9

Acknowledgements
Not applicable.

Author contributions
The study was conceptualized and designed by Biao Zhang, Bolin Zhang, Lijun Cen, and Zhizhou Wang. Biao Zhang and Tingxin Wang collected and analyzed data. Bolin Zhang and Bingqian Huang performed experiments. Biao Zhang and Bolin Zhang drafted the manuscript. Lijun Cen and Zhizhou Wang revised the manuscript.

Funding
Not applicable.

Data availability
Raw data and R codes for this study are available from the first and corresponding authors.

Declarations

Ethics approval and consent to participate
Not applicable.

Consent for publication
Not applicable.

Competing interests
The authors declare no competing interests.

Author details
[1]Department of General Surgery, The First Affiliated Hospital of Dalian Medical University, Dalian, Liaoning, China
[2]Department of Visceral, Vascular and Endocrine Surgery, Martin-Luther-University Halle- Wittenberg, University Medical Center Halle, Halle, Germany
[3]Institute (College) of Integrative Medicine, Dalian Medical University, Dalian, Liaoning, China
[4]Department of Transfusion Medicine, Affiliated Hospital of Youjiang Medical University for Nationalities, Baise, Guangxi, China
[5]Key Laboratory of Molecular Pathology in Tumors of Guangxi, Affiliated Hospital of Youjiang Medical University for Nationalities, Baise, Guangxi, China

Received: 27 August 2024 / Accepted: 25 October 2024
Published online: 01 November 2024

References

1. Miller KD, Nogueira L, Devasia T, Mariotto AB, Yabroff KR, Jemal A, et al. Cancer treatment and survivorship statistics, 2022. CA Cancer J Clin. 2022;72:409–36.
2. Kleeff J, Korc M, Apte M, La Vecchia C, Johnson CD, Biankin AV, et al. Pancreatic cancer. Nat Rev Dis Primers. 2016;2:16022.
3. Neoptolemos JP, Kleeff J, Michl P, Costello E, Greenhalf W, Palmer DH. Therapeutic developments in pancreatic cancer: current and future perspectives. Nat Rev Gastroenterol Hepatol. 2018;15:333–48.
4. Zhang B, Yuan Q, Zhang B, Li S, Wang Z, Liu H, et al. Characterization of neuroendocrine regulation- and metabolism-associated molecular features and prognostic indicators with aid to clinical chemotherapy and immunotherapy of patients with pancreatic cancer. Front Endocrinol. 2023;13:1078424.
5. Schawkat K, Manning MA, Glickman JN, Mortele KJ. Pancreatic ductal adenocarcinoma and its variants: pearls and perils. Radiographics. 2020;40:1219–39.
6. Neoptolemos JP, Palmer DH, Ghaneh P, Psarelli EE, Valle JW, Halloran CM, et al. Comparison of adjuvant gemcitabine and capecitabine with gemcitabine monotherapy in patients with resected pancreatic cancer (ESPAC-4): a multicentre, open-label, randomised, phase 3 trial. Lancet. 2017;389:1011–24.
7. Conroy T, Hammel P, Hebbar M, Ben Abdelghani M, Wei AC, Raoul J-L, et al. FOLFIRINOX or Gemcitabine as Adjuvant Therapy for Pancreatic Cancer. N Engl J Med. 2018;379:2395–406.
8. Tanaka M, Mihaljevic AL, Probst P, Heckler M, Klaiber U, Heger U, et al. Meta-analysis of recurrence pattern after resection for pancreatic cancer. Br J Surg. 2019;106:1590–601.
9. Hannun YA, Obeid LM. Sphingolipids and their metabolism in physiology and disease. Nat Rev Mol Cell Biol. 2018;19:175–91.
10. Green CD, Maceyka M, Cowart LA, Spiegel S. Sphingolipids in metabolic disease: the good, the bad, and the unknown. Cell Metabol. 2021;33:1293–306.
11. Xiao J, Lin H, Liu B, Xia Z, Zhang J, Jin J. Decreased S1P and SPHK2 are involved in pancreatic acinar cell injury. Biomark Med. 2019;13:627–37.
12. Lin M, Li Y, Wang S, Cao B, Li C, Li G. Sphingolipid metabolism and signaling in Lung Cancer: a potential therapeutic target. J Oncol. 2022;2022:1–10.
13. Zhu R, Xiao J, Luo D, Dong M, Sun T, Jin J. Serum AKR1B10 predicts the risk of hepatocellular carcinoma - A retrospective single-center study. Gastroenterol Hepatol. 2019;42:614–21.
14. Hannun YA, Bell RM. Lysosphingolipids inhibit protein kinase C: implications for the sphingolipidoses. Science. 1987;235:670–4.
15. Tumor necrosis factor. -alpha activates the sphingomyelin signal transduction pathway in a cell-free system. Science. 1992;255:1715–8.
16. Ogretmen B, Hannun YA. Biologically active sphingolipids in cancer pathogenesis and treatment. Nat Rev Cancer. 2004;4:604–16.

17. Pei S, Zhang P, Yang L, Kang Y, Chen H, Zhao S, et al. Exploring the role of sphingolipid-related genes in clinical outcomes of breast cancer. Front Immunol. 2023;14:1116839.
18. Ecker J, Benedetti E, Kindt ASD, Höring M, Perl M, Machmüller AC, et al. The Colorectal Cancer Lipidome: identification of a robust tumor-specific lipid species signature. Gastroenterology. 2021;161:910–e92319.
19. Zhang Y, Ji S, Zhang X, Lu M, Hu Y, Han Y, et al. Human *CPTP* promotes growth and metastasis via sphingolipid metabolite ceramide and PI4KA/AKT signaling in pancreatic cancer cells. Int J Biol Sci. 2022;18:4963–83.
20. Leek JT, Johnson WE, Parker HS, Jaffe AE, Storey JD. The sva package for removing batch effects and other unwanted variation in high-throughput experiments. Bioinformatics. 2012;28:882–3.
21. Zhang P, Pei S, Wu L, Xia Z, Wang Q, Huang X, et al. Integrating multiple machine learning methods to construct glutamine metabolism-related signatures in lung adenocarcinoma. Front Endocrinol. 2023;14:1196372.
22. Zhang B, Chen X, Wang Z, Guo F, Zhang X, Huang B, et al. Identifying endoplasmic reticulum stress-related molecular subtypes and prognostic model for predicting the immune landscape and therapy response in pancreatic cancer. Aging. 2023;15:10549–79.
23. Zhao S, Zhang X, Gao F, Chi H, Zhang J, Xia Z, et al. Identification of copper metabolism-related subtypes and establishment of the prognostic model in ovarian cancer. Front Endocrinol. 2023;14:1145797.
24. Zhang J, Peng G, Chi H, Yang J, Xie X, Song G, et al. CD8 + T-cell marker genes reveal different immune subtypes of oral lichen planus by integrating single-cell RNA-seq and bulk RNA-sequencing. BMC Oral Health. 2023;23:464.
25. Chi H, Xie X, Yan Y, Peng G, Strohmer DF, Lai G, et al. Natural killer cell-related prognosis signature characterizes immune landscape and predicts prognosis of HNSCC. Front Immunol. 2022;13:1018685.
26. Yoshihara K, Shahmoradgoli M, Martínez E, Vegesna R, Kim H, Torres-Garcia W, et al. Inferring tumour purity and stromal and immune cell admixture from expression data. Nat Commun. 2013;4:2612.
27. Newman AM, Liu CL, Green MR, Gentles AJ, Feng W, Xu Y, et al. Robust enumeration of cell subsets from tissue expression profiles. Nat Methods. 2015;12:453–7.
28. Maeser D, Gruener RF, Huang RS. oncoPredict: an R package for predicting *in vivo* or cancer patient drug response and biomarkers from cell line screening data. Brief Bioinform. 2021;22:bbab260.
29. Liang L, Yan J, Huang X, Zou C, Chen L, Li R, et al. Identification of molecular signatures associated with sleep disorder and Alzheimer's disease. Front Psychiatry. 2022;13:925012.
30. Yang H, Li Z, Zhu S, Wang W, Zhang J, Zhao D, et al. Molecular mechanisms of pancreatic cancer liver metastasis: the role of PAK2. Front Immunol. 2024;15:1347683.
31. Zhu C, Sun Z, Wang J, Meng X, Ma Z, Guo R, et al. Exploring oncogenes for renal clear cell carcinoma based on G protein-coupled receptor-associated genes. Discov Onc. 2023;14:182.
32. Wang J, Zuo Z, Yu Z, Chen Z, Tran LJ, Zhang J, et al. Collaborating single-cell and bulk RNA sequencing for comprehensive characterization of the bladder cancer intratumor heterogeneity and prognostic model development for bladder cancer. Aging. 2023;15:12104–19.
33. Zhang S, Jiang C, Jiang L, Chen H, Huang J, Gao X, et al. Construction of a diagnostic model for hepatitis B-related hepatocellular carcinoma using machine learning and artificial neural networks and revealing the correlation by immunoassay. Tumour Virus Res. 2023;16:200271.
34. Zhang B, Huang B, Zhang X, Li S, Zhu J, Chen X, et al. PANoptosis-related molecular subtype and prognostic model associated with the immune microenvironment and individualized therapy in pancreatic cancer. Front Oncol. 2023;13:1217654.
35. Zhang P, Pei S, Gong Z, Feng Y, Zhang X, Yang F, et al. By integrating single-cell RNA-seq and bulk RNA-seq in sphingolipid metabolism, CACYBP was identified as a potential therapeutic target in lung adenocarcinoma. Front Immunol. 2023;14:1115272.
36. Chandrashekar DS, Bashel B, Balasubramanya SAH, Creighton CJ, Ponce-Rodriguez I, Chakravarthi BVSK, et al. UALCAN: a portal for facilitating Tumor Subgroup Gene expression and survival analyses. Neoplasia. 2017;19:649–58.
37. Pontén F, Schwenk JM, Asplund A, Edqvist P-HD. The human protein atlas as a proteomic resource for biomarker discovery: review: the human protein atlas. J Intern Med. 2011;270:428–46.
38. Szklarczyk D, Gable AL, Lyon D, Junge A, Wyder S, Huerta-Cepas J, et al. STRING v11: protein–protein association networks with increased coverage, supporting functional discovery in genome-wide experimental datasets. Nucleic Acids Res. 2019;47:D607–13.
39. Yan J, Fang Z, Shi M, Tu C, Zhang S, Jiang C, et al. Clinical significance of disulfidptosis-related genes and functional analysis in gastric Cancer. J Cancer. 2024;15:1053–66.
40. Zeng Z, Li Y, Pan Y, Lan X, Song F, Sun J, et al. Cancer-derived exosomal mir-25-3p promotes pre-metastatic niche formation by inducing vascular permeability and angiogenesis. Nat Commun. 2018;9:5395.
41. Zhu Y, Chang S, Liu J, Wang B. Identification of a novel cuproptosis-related gene signature for multiple myeloma diagnosis. Immun Inflam Disease. 2023;11:e1058.
42. Stuart T, Butler A, Hoffman P, Hafemeister C, Papalexi E, Mauck WM, et al. Comprehensive Integration of Single-Cell Data. Cell. 2019;177:1888–e190221.
43. Ma B, Qin L, Sun Z, Wang J, Tran LJ, Zhang J, et al. The single-cell evolution trajectory presented different hypoxia heterogeneity to reveal the carcinogenesis of genes in clear cell renal cell carcinoma: based on multiple omics and real experimental verification. Environ Toxicol. 2024;39:869–81.
44. Zou D, Huang X, Lan Y, Pan M, Xie J, Huang Q, et al. Single-cell and spatial transcriptomics reveals that PTPRG activates the m6A methyltransferase VIRMA to block mitophagy-mediated neuronal death in Alzheimer's disease. Pharmacol Res. 2024;201:107098.
45. Mabbott NA, Baillie J, Brown H, Freeman TC, Hume DA. An expression atlas of human primary cells: inference of gene function from coexpression networks. BMC Genomics. 2013;14:632.
46. Li Z, Zhou H, Xia Z, Xia T, Du G, Franziska SD, et al. HMGA1 augments palbociclib efficacy via PI3K/mTOR signaling in intrahepatic cholangiocarcinoma. Biomark Res. 2023;11:33.
47. Ye Y, Zhao Q, Wu Y, Wang G, Huang Y, Sun W, et al. Construction of a cancer-associated fibroblasts-related long non-coding RNA signature to predict prognosis and immune landscape in pancreatic adenocarcinoma. Front Genet. 2022;13:989719.
48. Huang X, Chi H, Gou S, Guo X, Li L, Peng G, et al. An aggrephagy-related LncRNA signature for the prognosis of pancreatic adenocarcinoma. Genes. 2023;14:124.
49. Chen Q, Pu N, Yin H, Zhang J, Zhao G, Lou W, et al. CD73 acts as a prognostic biomarker and promotes progression and immune escape in pancreatic cancer. J Cell Mol Med. 2020;24:8674–86.
50. Yan J, Yu X, Li Q, Miao M, Shao Y. Machine learning to establish three sphingolipid metabolism genes signature to characterize the immune landscape and prognosis of patients with gastric cancer. BMC Genomics. 2024;25:319.
51. Ogretmen B. Sphingolipid metabolism in cancer signalling and therapy. Nat Rev Cancer. 2018;18:33–50.
52. Li R-Z, Wang X-R, Wang J, Xie C, Wang X-X, Pan H-D, et al. The key role of sphingolipid metabolism in cancer: New therapeutic targets, diagnostic and prognostic values, and anti-tumor immunotherapy resistance. Front Oncol. 2022;12:941643.
53. Cheng Y, Wang K, Geng L, Sun J, Xu W, Liu D, et al. Identification of candidate diagnostic and prognostic biomarkers for pancreatic carcinoma. EBioMedicine. 2019;40:382–93.
54. Chi H, Peng G, Wang R, Yang F, Xie X, Zhang J, et al. Cuprotosis programmed-cell-death-related lncRNA signature predicts prognosis and Immune Landscape in PAAD patients. Cells. 2022;11:3436.
55. Yuan Q, Deng D, Pan C, Ren J, Wei T, Wu Z, et al. Integration of transcriptomics, proteomics, and metabolomics data to reveal HER2-associated metabolic heterogeneity in gastric cancer with response to immunotherapy and neoadjuvant chemotherapy. Front Immunol. 2022;13:951137.
56. Ren Q, Zhang P, Lin H, Feng Y, Chi H, Zhang X, et al. A novel signature predicts prognosis and immunotherapy in lung adenocarcinoma based on cancer-associated fibroblasts. Front Immunol. 2023;14:1201573.
57. Zhang B, Liu J, Li H, Huang B, Zhang B, Song B, et al. Integrated multi-omics identified the novel intratumor microbiome-derived subtypes and signature to predict the outcome, tumor microenvironment heterogeneity, and immunotherapy response for pancreatic cancer patients. Front Pharmacol. 2023;14:1244752.
58. Pan C, Deng D, Wei T, Wu Z, Zhang B, Yuan Q, et al. Metabolomics study identified bile acids as potential biomarkers for gastric cancer: a case control study. Front Endocrinol. 2022;13:1039786.
59. Zhang B, Sun J, Guan H, Guo H, Huang B, Chen X, et al. Integrated single-cell and bulk RNA sequencing revealed the molecular characteristics and prognostic roles of neutrophils in pancreatic cancer. Aging. 2023;15:9718–42.
60. Wang H, Jin X, Zhang Y, Wang Z, Zhang T, Xu J, et al. Inhibition of sphingolipid metabolism in osteosarcoma protects against CD151-mediated tumorigenicity. Cell Biosci. 2022;12:169.

61. Malavaud B, Pchejetski D, Mazerolles C, De Paiva GR, Calvet C, Doumerc N, et al. Sphingosine kinase-1 activity and expression in human prostate cancer resection specimens. Eur J Cancer. 2010;46:3417–24.
62. Knapp P, Bodnar L, Błachnio-Zabielska A, Świderska M, Chabowski A. Plasma and ovarian tissue sphingolipids profiling in patients with advanced ovarian cancer. Gynecol Oncol. 2017;147:139–44.
63. Ruckhäberle E, Rody A, Engels K, Gaetje R, Von Minckwitz G, Schiffmann S, et al. Microarray analysis of altered sphingolipid metabolism reveals prognostic significance of sphingosine kinase 1 in breast cancer. Breast Cancer Res Treat. 2008;112:41–52.
64. Kawakita Y, Motoyama S, Sato Y, Koyota S, Wakita A, Liu J, et al. Sphingosine-1-phosphate/sphingosine kinase 1-dependent lymph node metastasis in esophageal squamous cell carcinoma. Surg Today. 2017;47:1312–20.
65. Li W, Yu C-P, Xia J, Zhang L, Weng G-X, Zheng H, et al. Sphingosine kinase 1 is Associated with gastric Cancer progression and poor survival of patients. Clin Cancer Res. 2009;15:1393–9.
66. Hu X, Zhou X, Zhang J, Li L. Sphingolipid metabolism is associated with osteosarcoma metastasis and prognosis: evidence from interaction analysis. Front Endocrinol. 2022;13:983606.
67. Zhang Y, Wang Y, Wan Z, Liu S, Cao Y, Zeng Z. Sphingosine kinase 1 and Cancer: a systematic review and Meta-analysis. PLoS ONE. 2014;9:e90362.
68. Zhang X, Zhang P, Cong A, Feng Y, Chi H, Xia Z, et al. Unraveling molecular networks in thymic epithelial tumors: deciphering the unique signatures. Front Immunol. 2023;14:1264325.
69. Han J, Zhang B, Zhang Y, Yin T, Cui Y, Liu J, et al. Gut microbiome: decision-makers in the microenvironment of colorectal cancer. Front Cell Infect Microbiol. 2023;13:1299977.
70. Liu J, Zhang B, Zhang G, Shang D. Reprogramming of regulatory T cells in inflammatory tumor microenvironment: can it become immunotherapy turning point? Front Immunol. 2024;15:1345838.
71. Anderson NM, Simon MC. The tumor microenvironment. Curr Biol. 2020;30:R921–5.
72. Gong X, Chi H, Xia Z, Yang G, Tian G. Advances in HPV-associated tumor management: therapeutic strategies and emerging insights. J Med Virol. 2023;95:e28950.
73. Weigert A, Tzieply N, Von Knethen A, Johann AM, Schmidt H, Geisslinger G, et al. Tumor Cell apoptosis polarizes macrophages—role of Sphingosine-1-Phosphate. MBoC. 2007;18:3810–9.
74. Nema R, Kumar A. Sphingosine-1-Phosphate catabolizing enzymes predict better prognosis in Triple-negative breast Cancer patients and correlates with tumor-infiltrating Immune cells. Front Mol Biosci. 2021;8:697922.
75. Jiang X, Xu J, Liu M, Xing H, Wang Z, Huang L, et al. Adoptive CD8 + T cell therapy against cancer:challenges and opportunities. Cancer Lett. 2019;462:23–32.
76. Sarvaria A, Madrigal JA, Saudemont A. B cell regulation in cancer and anti-tumor immunity. Cell Mol Immunol. 2017;14:662–74.
77. Downs-Canner SM, Meier J, Vincent BG, Serody JS. B cell function in the Tumor Microenvironment. Annu Rev Immunol. 2022;40:169–93.
78. Iglesia MD, Vincent BG, Parker JS, Hoadley KA, Carey LA, Perou CM, et al. Prognostic B-cell signatures using mRNA-Seq in patients with subtype-specific breast and ovarian Cancer. Clin Cancer Res. 2014;20:3818–29.
79. Iglesia MD, Parker JS, Hoadley KA, Serody JS, Perou CM, Vincent BG. Genomic analysis of Immune Cell infiltrates across 11 Tumor types. JNCI J Natl Cancer Inst. 2016;108:djw144.
80. Yang C, Lee H, Pal S, Jove V, Deng J, Zhang W, et al. B cells promote Tumor Progression via STAT3 regulated-angiogenesis. PLoS ONE. 2013;8:e64159.
81. Dong HP, Elstrand MB, Holth A, Silins I, Berner A, Trope CG, et al. NK- and B-Cell infiltration correlates with worse outcome in metastatic ovarian carcinoma. Am J Clin Pathol. 2006;125:451–8.
82. Zhai X, Xia Z, Du G, Zhang X, Xia T, Ma D, et al. LRP1B suppresses HCC progression through the NCSTN/PI3K/AKT signaling axis and affects doxorubicin resistance. Genes Dis. 2023;10:2082–96.
83. Xia Z, Chen S, He M, Li B, Deng Y, Yi L, et al. Editorial: targeting metabolism to activate T cells and enhance the efficacy of checkpoint blockade immunotherapy in solid tumors. Front Immunol. 2023;14:1247178.
84. Li R, Hao Y, Wang Q, Meng Y, Wu K, Liu C, et al. ECHS1, an interacting protein of LASP1, induces sphingolipid-metabolism imbalance to promote colorectal cancer progression by regulating ceramide glycosylation. Cell Death Dis. 2021;12:911.
85. Wang F, Wu Z. Sphingosine kinase 1 overexpression is associated with poor prognosis and oxaliplatin resistance in hepatocellular carcinoma. Exp Ther Med. 2018;15:5371–6.
86. Qiu Y, Yang S, Pan T, Yu L, Liu J, Zhu Y, et al. ANKRD22 is involved in the progression of prostate cancer. Oncol Lett. 2019;18:4106–13.
87. Pan T, Liu J, Xu S, Yu Q, Wang H, Sun H, et al. ANKRD22, a novel tumor microenvironment-induced mitochondrial protein promotes metabolic reprogramming of colorectal cancer cells. Theranostics. 2020;10:516–36.
88. Wu Y, Liu H, Gong Y, Zhang B, Chen W. ANKRD22 enhances breast cancer cell malignancy by activating the Wnt/β-catenin pathway via modulating NuSAP1 expression. Bosn J Basic Med Sci. 2021;21:294–304.
89. Yin J, Fu W, Dai L, Jiang Z, Liao H, Chen W, et al. ANKRD22 promotes progression of non-small cell lung cancer through transcriptional up-regulation of E2F1. Sci Rep. 2017;7:4430.
90. Liu K, Cui L, Li C, Tang C, Niu Y, Hao J, et al. Pan-cancer analysis of the prognostic and immunological role of ANLN: an onco-immunological biomarker. Front Genet. 2022;13:922472.
91. Zhang X, Li L, Huang S, Liao W, Li J, Huang Z, et al. Comprehensive Analysis of ANLN in Human tumors: a prognostic Biomarker Associated with Cancer Immunity. Oxidative Med Cell Longev. 2022;2022:1–14.
92. Ding G, Lu W, Zhang Q, Li K, Zhou H, Wang F, et al. ZBTB38 suppresses prostate cancer cell proliferation and migration via directly promoting DKK1 expression. Cell Death Dis. 2021;12:998.
93. Hall CL, Daignault SD, Shah RB, Pienta KJ, Keller ET. Dickkopf-1 expression increases early in prostate cancer development and decreases during progression from primary tumor to metastasis. Prostate. 2008;68:1396–404.
94. Betella I, Turbitt WJ, Szul T, Wu B, Martinez A, Katre A, et al. Wnt signaling modulator DKK1 as an immunotherapeutic target in ovarian cancer. Gynecol Oncol. 2020;157:765–74.
95. Shi T, Zhang Y, Wang Y, Song X, Wang H, Zhou X, et al. DKK1 promotes Tumor Immune Evasion and impedes Anti–PD-1 treatment by inducing immunosuppressive macrophages in gastric Cancer. Cancer Immunol Res. 2022;10:1506–24.

Publisher's note